1-1-2015

Analysis And Suppression Of Engine Hood Vibrations Under Random Road Excitations

Hooman Farrokhzadeh
Wayne State University,

ANALYSIS AND SUPPRESSION OF ENGINE HOOD VIBRATIONS UNDER RANDOM ROAD EXCITATIONS

by

HOOMAN FARROKHZADEH

THESIS

Submitted to the Graduate School

of Wayne State University,

Detroit, Michigan

in partial fulfillment of the requirements

for the degree of

MASTER OF SCIENCE

2015

MAJOR: MECHANICAL ENGINEEIRNG

Approved By:

_____

Advisor Date

ACKNOWLEDGMENTS

I hereby place my deep sense of gratitude to my adviser, Professor Chin-An Tan, for providing me with support and mentorship to carry out this task. I am also very thankful to the committee members, Dr. Eamon and Dr. Ayorinde to specify a time for my work during their busy schedule.

I would also like to express my sincere gratitude to Professor Trilochan Singh for all his advice and guidance during my studying. I convey my sincere thanks to my family, all my friends at Wayne State University and the company I am working for, without whose co-operation this step would not have been a success.

TABLE OF CONTENTS

LIST OF TABLES

LIST OF FIGURES

CHAPTER 1 INTRODUCTION

1.1 Background and Motivation

One of the most important issues to be considered in vehicle design is meeting the safety legislations. Head injury is the most common reason of fatalities in vehicle-pedestrian crashes. The engine hood plays the most important role in this regards. There are two main ways to improve the performance of a hood panel with respect to the pedestrian safety, namely, changing the structure and the parameters. Any change in the outer hood panel such as the curvature must be consistent with the entire physique of the vehicle. Therefore, the most effective variable for the optimization of the crash performance of a vehicle is the panel thickness. On the other hand, the increasing demand for lower fuel consumption while maintaining a good acceleration performance, leads to reducing the weight of a vehicle by reducing the thickness of panels as well as utilization of non-traditional materials in the structure. Due to the larger volume of the engine hood compared with other components, it is one of the targets for weight reduction. However, by addressing all of the above-mentioned issues, the engine hood panel will be more susceptible to vibrations [1-3].

Hood vibrations are mainly caused by fluid-structure interactions due to the aeroelasticity also known as the flutter phenomenon, and base excitations, resulting from the road surface irregularities. Hood flutter was extensively investigated in the past [1, 2].However, to the author's best knowledge, not enough attention has been given to the vibrations stemming from surface roughness. With the aim of discussing the effect of surface roughness on vehicle vibrations, this work proposes a method to analyze the hood

vibrations problem and suppress the resultant response amplitude.

1.2 Objectives

Experimental Modal Analysis (EMA) and Computer Aided Engineering, CAE are the most useful tools for precise investigation of the engine hood vibrations. The very first objective of this work is to develop a reliable model for hood panel using the Finite Element Method, FEM. This model will be validated with the Experimental Model Analysis. Secondly, random vibrations analysis will be performed to find the response of the structure to the excitations from road unevenness. MSC NASTRAN will be utilized for processing of random vibrations analysis. Subsequently, after finding the response of the engine hood under random excitations, third objective will be to suppress the vibration levels at a designated point on the structure.

1.3 Organization

This thesis is organized into six chapters, as described below:

Chapter 1 introduces the background and motivation of this research as well as the overall objectives and organization of the thesis. Chapter 2 includes a literature review on the main areas of interest. This chapter begins with introducing the experimental, analytical, and CAE approaches on random road excitations. Focus is then allocated to the validation of CAE models in studying the dynamic characteristics of car components; and finally the common methods to reduce noise and vibration levels in automotive industry are presented.

In Chapter 3, the dynamic characteristics of hood structure are extracted via CAE and EMA. In this Chapter, the obtained results are compared to evaluate the accuracy of the

CAE model. The methods and results are compared with the findings reported in the literature published in SAE aiming at dynamics characterization of the car hood flutter.

Chapter 4 starts with background and concepts of random vibrations analysis in CAE, followed by presentation of the input data gained from actual road conditions and finally the results obtained from the response of hood structure to random road excitation are described in detail. In Chapter 5, a technique is presented to suppress the amplitude of hood response under road base excitations. Consequently, in Chapter 6 the conclusions drawn from this work are presented along with suggestions towards future research in this area.

CHAPTER 2 LITERATURE REVIEW

This chapter is divided into three sections. In the first section the road unevenness profile will be discussed. Due to their random distribution pattern, the road surface irregularities are categorized as a random process. The analytical models that describe this process as well as the common methods for measurement of the road surface profiles are discussed in this section. The second section encompasses the application of CAE and Experiment in extracting dynamic characteristics of car components. For this purpose, vehicle door panel, fuel tank engine hood structure, and weather-strips will be reviewed. Finally the methods commonly used in the automotive industry to reduce vibration levels will be summarized.

2.1 Random base excitation due to road surface irregularities

Powertrain and wheels are significant sources of moving vehicle vibrations. Due to the development of less noisy powertrains, the main source of noise and vibrations in cars is excitation coming from the road surface unevenness [4-7]. The interactions between the road irregularities and tire treads create vibrations that propagate through the tire and generate air-borne noise[8]. Rolling noise[1] of cars and trains are generally due to the road roughness by irregularities of the running surfaces of the tread and the surface on which the wheel rolls. The surface roughness results in vertical vibrations in the vehicle structure [9]. In heavy articulated vehicles, both low and high frequency modes are excited which result in vibrations in all directions [10].

[1] In railway traffic, Rolling noise results from travelling speed of 40-250 km/h. (http://www.plassertheurer.com)

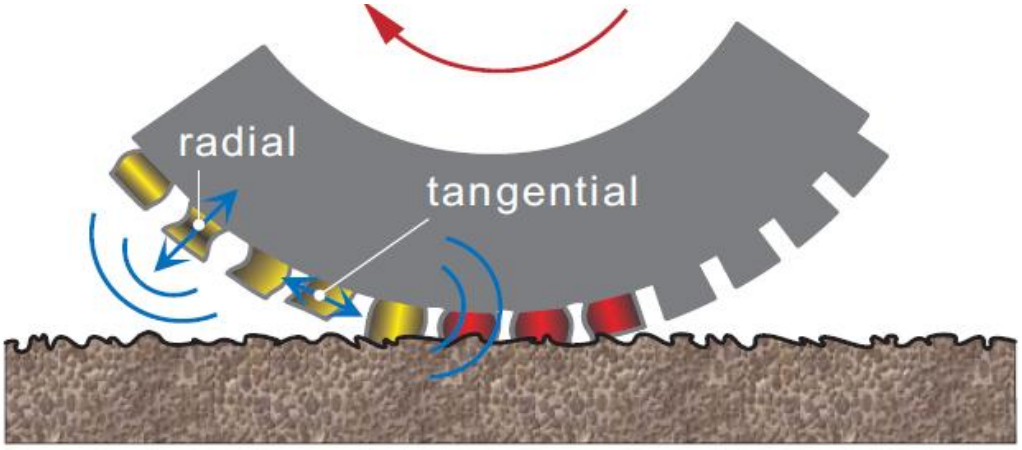

Figure 1: Radial and Tangential tire vibrations are the cause of tire/road noise [8]

The Exact description of road surface profile is an important step in vehicle development. It is influential in various aspects of vehicle engineering such as ride, comfort, chassis design, fatigue, and durability [4, 6, 7, 11-13].

Despite nonlinear and random characteristics of road excitations, cosine and sine waves are occasionally used to represent road excitations [14, 15]. Kropac and Mucka [14] simulated the effects of obstacles such as bumps and potholes on the vehicle response using cosine waves. The road unevenness is a random variable and its properties vary with the type of road surface [5]. A random process is often described with probability statistics method [4]. The power spectral density[2] (PSD) is widely used to describe the road characteristics. The road surface irregularities have two main components; steady-state and

[2]If the probability distributions remain unchanged in time the process is called stationary. In a stationary process, the power spectral density is the Fourier transform of autocorrelation. function $S(\omega) = \frac{1}{2\pi}\int_{-\infty}^{+\infty} R(\tau)e^{-i\omega\tau}d\tau$ [16]

transient. A combination of transient (fluctuations in root-mean square (RMS)[3] level [16]) and steady state components shows the non-stationary behavior of surface profiles [17]. In order to simulate random vibrations of vehicle in laboratory, the average PSD of the measured vibrations data is used. Garcia et al. [16] observed that there is no change in the shape of the PSD within the duration of each transport event. However, under the assumption that the velocity is constant, the surface irregularity can be assumed as a stationary random process [4, 9, 18, 19]. Road irregularities have been described as a Gaussian random process[4] by many researchers [6, 16, 17, 20-23]. Furthermore, the road unevenness can be approximated by a white noise[5] excitation process on the velocity level [9, 18, 22, 23].

Schiehlen [9] studied the influence of random road profiles based on the white noise excitation on the vertical dynamics of vehicles. The effect of random road excitations on harvesting power in dual mass energy harvesters[6] (e.g., regenerative vehicle suspensions) were investigated by Tang and Zuo [24]. They found that under the white noise random velocity excitation of road irregularities, the harvesting power gained from vehicle suspensions is proportional to the tire stiffness and the road vertical excitation spectrum. That is to say, sprung and unsprung mass, suspension damping coefficient and stiffness do

[3] The RMS value of a set of values (or a continuous-time waveform) is the square root of the arithmetic mean (average) of the squares of the original values (or the square of the function that defines the continuous waveform)

[4] The graph of a Gaussian probability density function is a bell-shaped curve and symmetric about the mean value. The probability density function of a Gaussian process $x(t)$ is given by

$p(x) = \frac{1}{\sqrt{2\pi}\sigma_x} e^{\frac{-1}{2}\left(\frac{x-\bar{x}}{\sigma_x}\right)^2}$ [16]

[5] White noise is the process that power spectral density is unchanged over a frequency range [16]

[6] A Vibration energy harvester is a spring-mass system with an electromagnetic or piezoelectric transducer connected in parallel with a spring [25].

not influence the harvesting power. Xu et al. [20] derived a sensitivity analysis[7] formula to optimize the vehicle suspension systems based on Gaussian assumption.

Pseudo Excitation Method (PEM) is extensively applied in simulating road conditions. In this method a random multi-excitation process is turned into a series of deterministic harmonic excitation [20, 21, 25-27]. Qin et al. [26] found that constructing six-wheel road PEM and obtaining PSD of responses are convenient for heavy-duty trucks. Xu et al. [21] used a Gaussian random process and PEM with a linear dynamic model to get the dynamic response of car.

Cyclostationary is a type of non-stationary random excitation in which the statistical properties change periodically with time. Jha et al. [28] found that the road concrete slabs with constant length are cyclostationary. This could give a more accurate estimation of the RMS of the response compared with the traditional stationary models. Lu et al. [19] suggested a computational model for random vibration analysis of the vehicle track system based on PEM and symplectic[8] methods. Cryer et al. [29] developed a road simulator for heavy duty vehicles to provide vertical inputs to the tire with respect to the conditions pertaining to this category of vehicles. The introduced system needed PSD matrix and particular measured road.

2.1.1 Analytical models for road profile

The road PSD is correlated with the vehicle speed. The road unevenness spectrum can

[7] Sensitivity analysis is the study of how the uncertainty in the output of a mathematical model or system (numerical or otherwise) can be apportioned to different sources of uncertainty in its inputs.(Wikipedia.com)

[8] This is a method to solve wave propagation problems for a periodic structure [[19] Lu, F., Kennedy, D., Williams, F. W., and Lin, J. H., 2008, "Symplectic analysis of vertical random vibration for coupled vehicle-track systems," Journal of Sound and Vibration 317(1-2), pp. 236-249.

be simply described with one-sided power spectral density (PSD)[9] [6, 9, 13].

$$\varphi_z(\Omega) = \varphi_0(\frac{\Omega_0}{\Omega})^w \, , 0 < \Omega_1 \leq \Omega \leq \Omega_2 < \infty \tag{2.1}$$

In the above-mentioned equation, Ω_0 is a standardized (reference) spatial circular frequency or angular spatial frequency [6] in rad/m and is usually estimated at 0.1 m^{-1} [13]. φ_0 is the unevenness index [6] which characterizes the roughness as a function of the spatial frequency Ω_0. Ω_1 and Ω_2 are the upper and lower bounds of the effective frequency band, respectively. For example for a B-level road, $\varphi_0 = 64E - 6\mathrm{m}^2$ .m $\Omega_1 = 0.01\mathrm{m}^{-1}$ and $\Omega_2 = 10\mathrm{m}^{-1}$.

The roughness level can be considered as an unevenness index and the waviness parameter or the waviness of road profile is represented by *w* such that the greater the *w*, the longer the wavelength. The waviness is found to be in the range of 1.75 < *w* < 2.25 with an average value of 2. Wavelength is described as $\lambda = \frac{2\pi}{\Omega}$, where$\Omega$ is the wavenumber [9]. This equation is usually plotted on a $\varphi - \Omega$ diagram (Figure 2) with double logarithmic scale which results in decline lines with slopes of *(−2w).*

[9] Two and one sided spectra illustration [16]

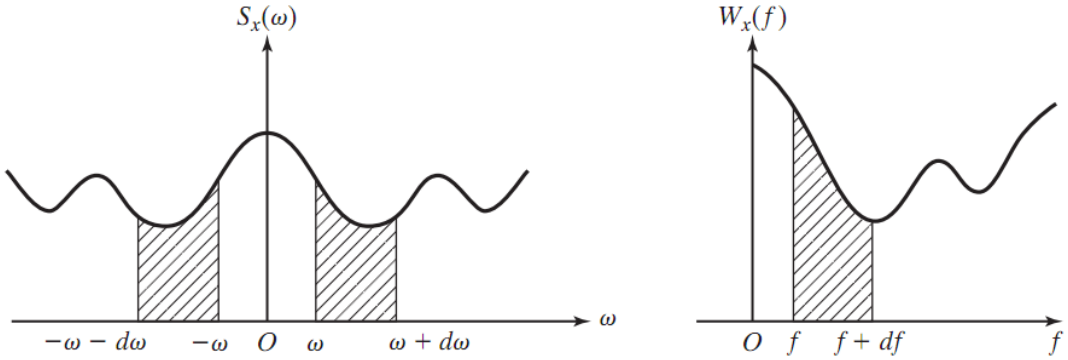

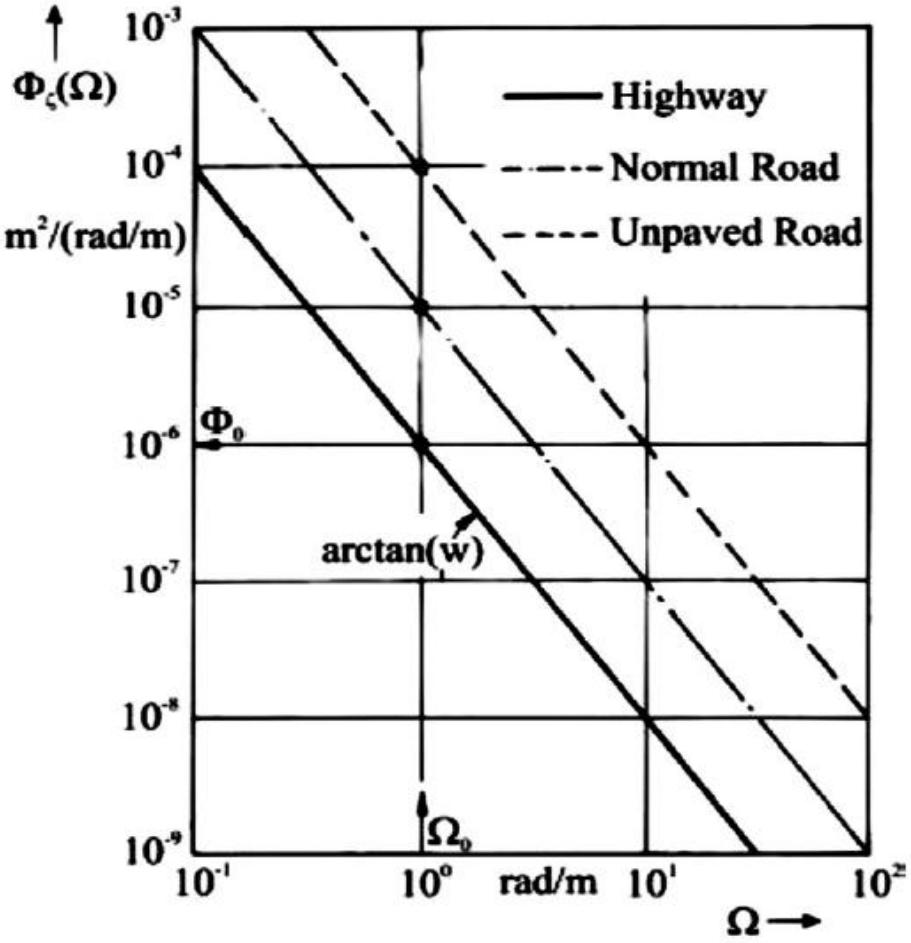

Figure 2: power spectral desnity of roads with a waviness factor [9].

The road irregularities can be expressed in a more complicated form as [9]:

$$\varphi_z(\Omega) = \begin{cases} \varphi_0(\frac{\Omega_0}{\Omega})^{w_1}, for\ 0 < \Omega_I \leq \Omega \leq \Omega_0 \\ \varphi_0(\frac{\Omega_0}{\Omega})^{w_2}, for\ \Omega_0 \leq \Omega \leq \Omega_{II} < \infty \end{cases} \quad (2.2)$$

Where, the different values of waviness $w_1, w_2,\ w_1 < w_2$ occur in two frequency ranges. Excitation *ζ(t)* in terms of displacement coming from road unevenness in time domain can be derived by the following equation:

$$\xi = v\tau \quad (2.3)$$

Where, τ is the correlation time corresponding to the correlation width ξ and ω in rad/s is the temporal circular frequency [9]. PSD of the vehicle excitation can be described by:

$$\varphi_{\xi}(\omega) = \frac{1}{v}\varphi_z \tag{2.4}$$

PSD of vertical road velocity and acceleration are [9, 18]:

$$\varphi_{\dot{\xi}}(\omega)=\omega^2\varphi_{\xi}(\omega) = 4\pi^2 G_q(n_0)n_0^2 V \tag{2.5}$$

$$\varphi_{\ddot{\xi}}(\omega)=\omega^4\varphi_{\xi}(\omega) =1\ 6\pi^4 G_q(n_0)n_0^2 V f^2 \tag{2.6}$$

As can be seen, constant velocity leads to constant PSD of the road profile. Mucka [6] studied the influence of random road profile waviness on the dynamic road loads. He used a quarter car model and displacement PSD with waviness of 1.5 to 2.5. Thus the constant waviness parameter assumption is capable of affecting the predicted random response.

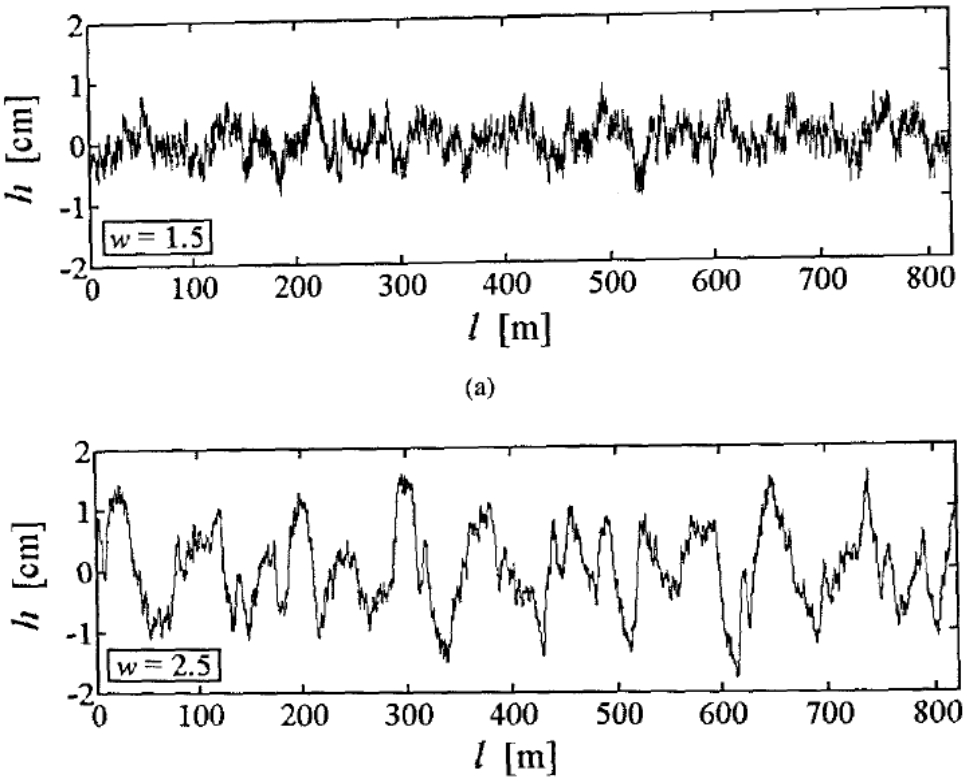

Figure 3: Longitudinal Road Profile with different waviness [6]

Through a subjective assessment survey, Hassan and Mc Manus [30] found that wavelengths in the range of 4.88 to 19.5 m, which lead to low frequency body vibration, are the most problematic in drivers' comfort issue. Kropac and Mucka [10] combined two fundamental properties of road PSD profile (unevenness index and waviness) into a single number. This method gives a more accurate vibration response and can be an extension to the road classification according to the ISO 8608[10]. Kropac and Mucka [14] used straightedge measurement to estimate PSD parameters, waviness and unevenness and Kuijpers studied the effect of roughness to rolling noise [8].

[10] ISO 8608 describes a uniform method of reporting measured vertical surface profile data from streets, roads, highways and off-road terrain. Measurement methods and measurement equipment are not included.(www.iso.org)

The road PSD can also found by writing motion equations for a Two-Degree-Of-Freedom system. The road profile is used as the system input, the transfer function is defined as PSD of acceleration of unsprung mass over road acceleration, the discrete acceleration signals in time domain are found and finally the PSD of unsprang mass is calculated to estimate the road PSD [18].

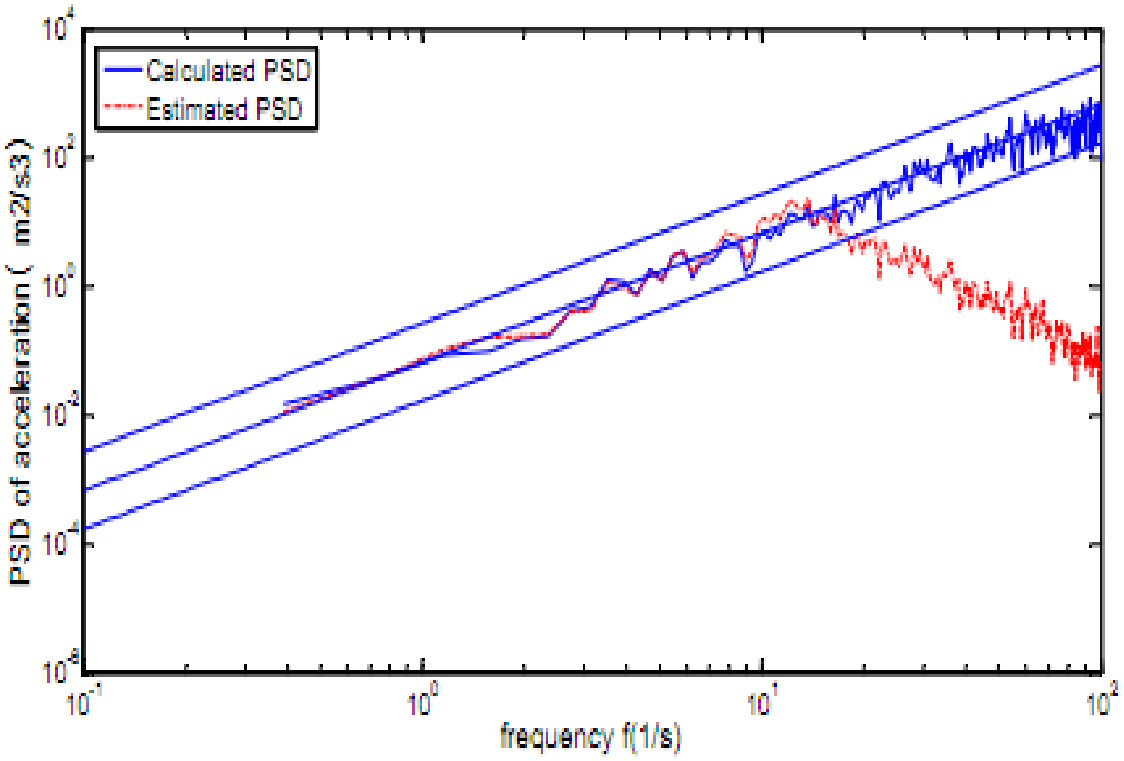

Figure 4: PSD Comparison between calculated and estimated road [18].

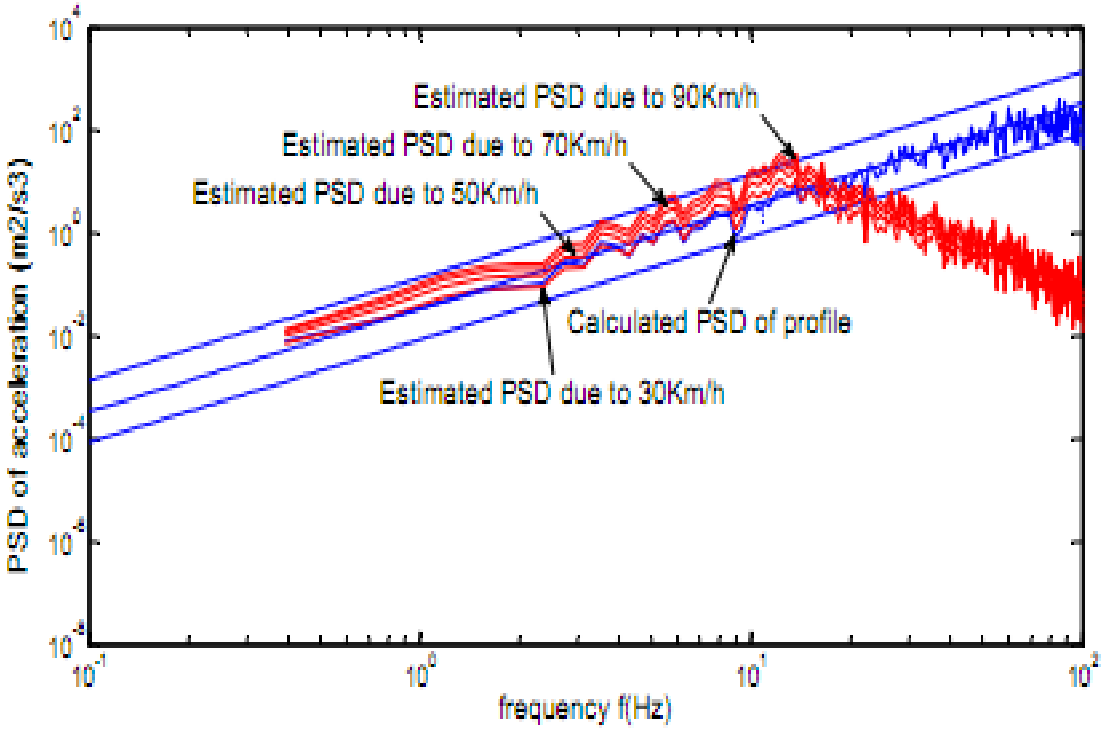

Figure 5: PSD comparison in different velocities [18].

Hassan and Mc Manus [30] used the roughness contents to develop a new index called "profile index for truck" (PIt). Accordingly, PIt of more than 2.75 m/km is perceived as a poor driveability. It was claimed that PIt works better in predictions of ride in heavy vehicles the IRI. Hesami and Mc Manus [31] found that wavelet based road profile analysis works better than PSD in terms of pavement roughness. It gives information about road roughness along with ability to check high frequency location such like potholes and cracks. They verified this approach with two experiments in 100 meter length of smooth and rough highway. Delanne and Pereira [32] compared three road profile signal processing methods to indicate road unevenness. Three criteria of international roughness index (IRI), PSD, and constant percent bandwidth spectrum analysis were studied. They found that IRI works well in terms of road conditions

assessment, road maintenance and repair service and road service level. When it comes to rehabilitation work and detecting impending problems on road sections, IRI is not the best choice and PSD is more appropriate in unevenness level evaluation. The conditions for validity of PSD are stationary stochastic process with a single regression line fitted. The road defects can be also found with PSD. Constant percent bandwidth spectrum analysis is useful in road service evaluation and detecting upcoming troubles with road sections.

2.1.2 Analytical modeling of vehicle

In theory of vehicle dynamics, vehicles are modelled as mechanical systems with mass, damping and stiffness which results in ordinary differential equations [9, 21]. The linear vehicle dynamic models under random road profiles are widely used to find dynamic response of the cars [13, 18, 21-23, 33, 34]. Among them a quarter vehicle model is the most reliable scale for road roughness condition [34], which is basically a 2 degree-of-freedom suspension system [6].

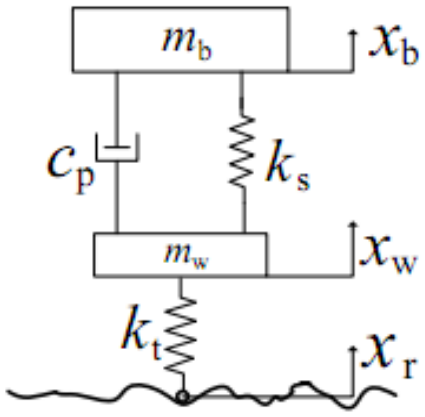

Figure 6: Quarter vehicle is modeled as a 2 degree-of-freedom suspension system [18]

In linear analytical study, the system is a mass-damping-stiffness model, the input is base excitation of road surface and the output can be acceleration at the point of interest. Transfer function from source to receiver and also dynamic loads can be achieved [22, 33]. Road PSD can be used as an input for the vehicle model [35]. Zhang and Jiang [22] found the optimal spring stiffness and viscous damping coefficient for obtaining the maximum reliability of SDOF and TDOF under random base excitations. If the acceleration is greater than the prescribed value, the failure will occur. Barbosa [36] on 2011, found FRF of a half-car-model under pavement roughness excitations. He found that the vehicle suspension mode is magnified at low speeds and at 120 km/h what makes passenger discomfort is the first vehicle mode in an undulated asphalted road. The optimization of a linear SDOF model system under stationary-zero mean Gaussian random excitation was studied by Dahlberg [23]. Gillespie and Karamihas [34] investigated important factors in developing a simplified dynamic model for truck response to road roughness inputs.

The human subjective perception is a function of acceleration response. Sujitamo [35] used a Four-degree-of freedom dynamic model and input of road roughness profile to find an output of human perception variable according to ISO 2631[11]. Most bodywork of vehicles can be modeled analytically by curved plates. Based on the theory of curved plates, a median surface is defined and two surfaces at equal distances from the median surface define the geometry of the plate. Car hood can be modeled accordingly [37].

Finite Element Method (FEM) is a powerful tool in random road vibrations analysis

[11] ISO 2631 The primary purpose of this part of ISO 2631 is to define methods of quantifying whole-body vibration in relation to human health and comfort, the probability of vibration perception and the incidence of motion sickness.

and is widely used by researchers [4, 5, 13, 38, 39]. Wu and Fan [38] established a mathematical and finite element model of 10 DOF to describe the vibrations of a truck. Rustighi et al. [5] used a three-dimensional elemental approach to predict the stochastic tire vibration. The non-linearities in contact model were not considered and experimental validations were also required. Through development of a precise FEM of tire, Low frequency road noise in a steady state conditions was modeled by Kido [39]. Quinman and Yonghani [4] used ANSYS for modal analysis and random vibration simulation of a truck transmission frame.

2.1.3 Measuring road roughness

Roughness is measured directly by getting PSD of road profile or indirectly by determining the sound pressure or the vibrations response level [8, 40]. The amplitude and frequency of perceived vibrations or sound are directly related to the roughness amplitude and wavelength.

2.1.3.1 Direct method

ISO 13473 describes the measurement instrumentation and data processing of direct road roughness measurements. Measurement of road profile systems can be static or dynamic. In a static format, a transducer is installed on a subframe and moves along a rigid beam. In the dynamic method, a laser source is mounted on a driving vehicle which collects the profile [7, 8, 12, 18]. Multiple laser profile sensors can improve test accuracy [12, 17]. Munari et al. [41] proposed that it is possible to use PSDs to generate new profiles without new measurements. However, the reliability of reconstructing terrain from PSDs should be assessed.

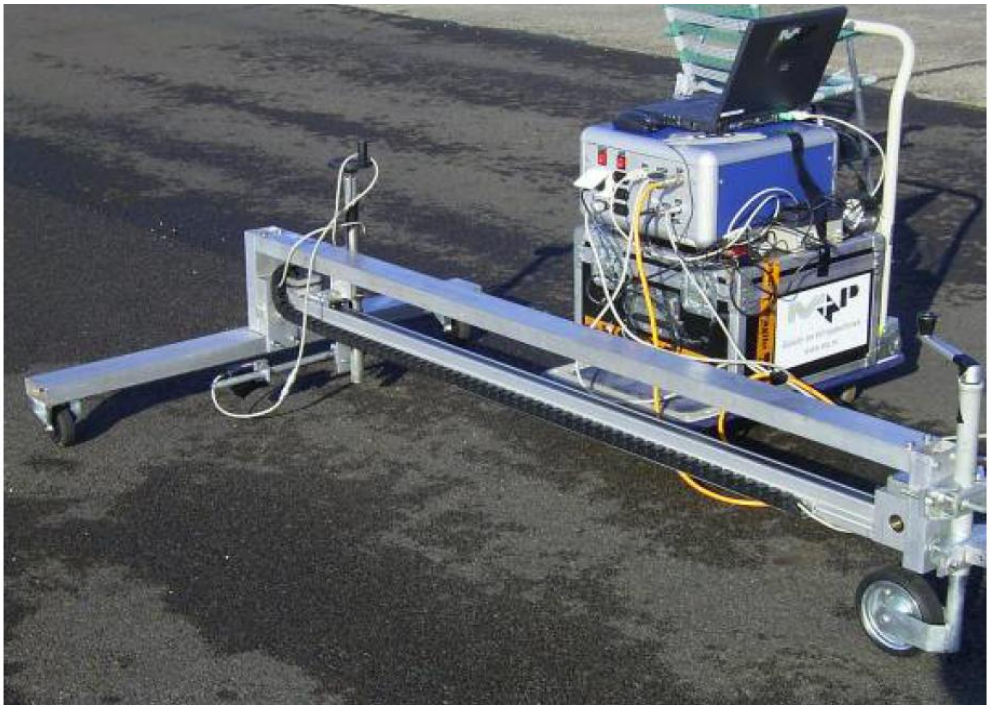

Figure 7: M+P static (3D) road surface roughness measurement system [8]

Acoustical transducers can be used to assess road roughness profile with fast roughness detection procedure. Xu et al. [42] found that in low frequency band which linear PSD may not be true, this method works well. Visual observations and profile based indexes are used in Australia to assess road pavement condition. PSD gives roughness information for specific longitudinal wavelength. Mann et al. [43] analyzed and compared rough and smooth sections of road from a laser profiler with IRI and PSD. They found that smooth pavements after construction have wavelengths greater than 35 m while wavelength of 2 m and less indicate pavement surface failure.

2.1.3.2 Indirect method

Previously, highway engineers measured suspension stroke to see the road roughness intensity. A modern approach is to simulate the response of vehicle to the road profile [17, 33, 34]. The

characteristics of vibration patterns produced by various road surface profiles can be found by determining vertical accelerations of the sprung and unsprung sides in a constant velocity [44]. Lakusic et al. [7] reported that the amplitude of car vibrations in cobblestone pavement is four times of asphalt pavement track. They recorded vibrations of between 40-80 km/h with accelerometers.

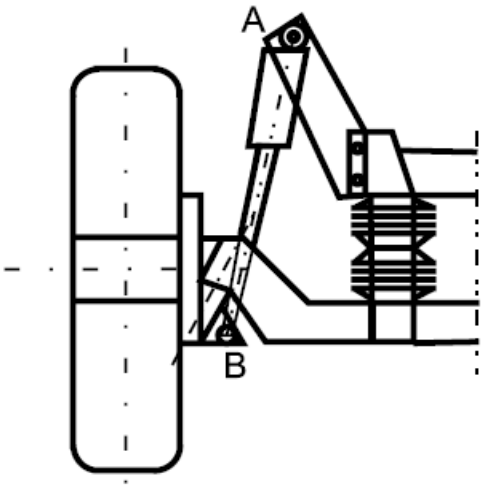

Figure 8: Locations of installing accelerometers [18].

The more corrugations on the road profile, the stronger the response of the vehicle. This is the reason why the response of the vehicle subjected to the sett[12] type of road profile is stronger. The car suspension works as a low–pass filter decreasing amplitudes more at higher frequencies. The signal generated by a rough road surface after passing through the suspension is noisier. Higher frequency excitations from the road profile are more important at higher velocities [44].

[12] A sett, usually referred to in the plural and known in some places as a Belgian block, is a broadly rectangular quarried stone used for paving roads.

2.2 Dynamic characterization of car components

Dynamic characterization of vehicle structures is an essential part in NVH analysis and helps a lot in refining noise and vibration in new vehicles. The main objective in this field is to find the correlation between the analytical, numerical and experimental results.

Different CAE[13] computer packages such as ANSYS, ADAMS, DADS, MSC Patran/MSC Nastran, Abaqus and IDEAS are used to develop the virtual model of vehicles [45]. It is common to evaluate the accuracy of numerical results obtained from CAE by comparing with experimental results. In case of anisotropic materials like fiber reinforced polymers or complex design as in vehicle components, verification of CAE simulations are more important [46]. Many researchers focused on CAE validation by methods like EMA and Image correlation of car components like hood, door panels and fuel tank in their works [46, 47]. Due to the inaccuracy of the boundary conditions simulation and also differences in scattering of the real properties of the structure, natural frequencies from EMA are always lower than those of CAE [47].

In modal analysis, mass density and material stiffness are the most dominating factors. So even a small change in these parameters results in a huge shift in natural frequencies. The modulus of elasticity of plastic materials is not directly measurable. Saravanan and Injeti [48] validated a FEM of car fuel tank with experiments. They determined the elasticity modulus of the plastic material through three point bending

[13] Computer-aided engineering (CAE) is the broad usage of computer software to aid in engineering analysis tasks. It includes Finite Element Analysis (FEA), Computational Fluid Dynamics (CFD), Multibody dynamics (MBD), and optimization. (Wikipedia.com)

tests[14] (ISO 178[15]). The CAE model of empty tank shows better correlation with test data. Liquid fuel is modeled as Non Structural Mass[16] (NSM) distributed over the tank shell structure. It was observed from CAE analysis that the vibration characteristics of gas tank are sensitive to the mass distribution of the liquid fuel inside the tank and also thickness of the tank.

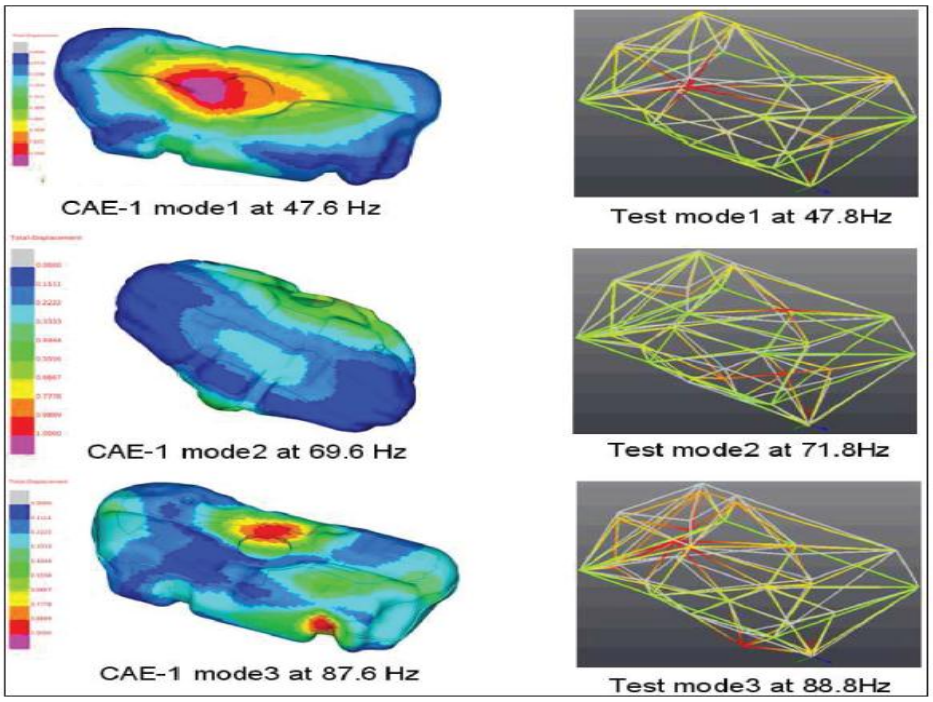

Figure 9: Modal analysis of fuel tank [48]

[14] The three points bending flexural test provides values for the modulus of elasticity in bending , flexural stress , flexural strain and the flexural stress-strain response of the material. The main advantage of a three point flexural test is the ease of the specimen preparation and testing. However, this method has also some disadvantages: the results of the testing method are sensitive to specimen and loading geometry and strain rate.

[15] ISO 178:2010 specifies a method for determining the flexural properties of rigid and semi-rigid plastics under defined conditions. A standard test specimen is defined, but parameters are included for alternative specimen sizes for use where appropriate. A range of test speeds is included. The method is used to investigate the flexural behavior of the test specimens and to determine the flexural strength, flexural modulus and other aspects of the flexural stress/strain relationship under the conditions defined. It applies to a freely supported beam, loaded at mid-span (three-point loading test).(www.iso.org)

[16] NSM are used to define masses that affect the behavior of specific element types but are not directly part of the structure of the model. (mscsoftware.com)

Hanouf et al. [45] extensively investigated the dynamic properties of door and hood panels of a car using CAE and EMA. Similarities were observed in frequencies and mode shapes. They used VPG 3.2 and LS DYNA for the CAE part and ME'scope VES for signal processing of EMA. An impact hammer, two FFT analyzers with 7 channels and six accelerometers were the equipment for experiment.

In order to improve the hood performance in crashes, car companies need to design more flexible panels. This flexibility in design results in undesirable vibrations of the hood at highway speeds. Furthermore, demands for reducing mass of body panels and decrease in component thickness, increases problems due to the increased sensitivity to aerodynamic loads. Transient CFD techniques coupled with CAE are capable of predicting how wind profiles influence the hood vibration. Expectedly, as the frequency of the oncoming flow approaches the natural frequencies of the hood, the response amplitude of the hood structure is the greatest in value. It was found that the turbulence grid (120 mph) produces the largest vibration. Hood flutter[17] with respect to aeroelasticity and fluid structure interaction (FSI) was extensively studied by Gaylard et al. [1] and Gupta et al. [2]. Aerodynamic loads are found with CFD solvers and potential conditions to generate vibrations were simulated using Lattice-Boltzmann Method (LBM). There are conditions which are found on road but are not easy to simulate in wind tunnel. Disturbed wind profiles such as those caused by high speed wakes, high speed travel at substantial yaw angles, and wind gusts are some of these conditions.

[17] A formal definition of aeroelastic flutter is a dynamic instability of a flight vehicle associated with the interaction of aerodynamic, elastic, and inertial forces [49] Hodges, D. H., and Pierce, G. A., 2011, Introduction to structural dynamics and aeroelasticity, Cambridge University Press, New York, NY..

Optical full field measurement[18] techniques are widely used for analysis of vibrations and mode shapes. Techniques such as Digital Speckle Pattern[19], Interferometry[20], Moiré[21], thermography or Photoelasticity[22] and the Digital Image Correlation (DIC)[23] have been successful in accurate measurement of the displacement [46, 47]. Two cameras capture the measurement field from different directions to find the three-dimensional contour of the designated area so whole displacement field is visualized. This technique possesses high resolution in space and time and as it determines the absolute position and displacement of the component, large amplitudes and rigid body movements can be found. By Digital Image Correlation (DIC) method and high speed cameras non-linear dynamic events can be analyzed and three-dimensional displacement field can be found.

Lampas et al. [46] combined optical measurements and computational techniques to simulate a non-linear transient dynamic event. Siebert et al. [47] investigated the deformation of a hood panel with Optical full field measurement techniques. The bonnet structure was loaded by a shaker with noise excitation for a classic experimental modal analysis. After dividing the structure into several points, each object point must be seen by both cameras at the same time. However, due

[18] In full-field optical methods light beams are used to illuminate and create images of the objects of interest. http://nam.epfl.ch/

[19] A speckle pattern is an intensity pattern produced by the mutual interference of a set of wave fronts distribution

[20] Interferometry is a family of techniques in which waves, usually electromagnetic, are superimposed in order to extract information about the waves.

[21] a secondary and visually evident superimposed pattern created when two identical patterns on a flat or curved surface are overlaid while displaced or rotated a small amount from one another

[22] Photoelasticity is an experimental method to determine the stress distribution in a material. The method is mostly used in cases where mathematical methods become quite cumbersome. Unlike the analytical methods of stress determination, Photoelasticity gives a fairly accurate picture of stress distribution, even around abrupt discontinuities in a material

[23] Digital Image Correlation, DIC, Digital image correlation and tracking is an optical method that employs tracking and image registration techniques for accurate 2D and 3D measurements of changes in images. This is often used to measure deformation, displacement, strain, and optical flow.

to the physique of the hood, not all points can be captured by cameras.

Figure 10: Setup of High speed DIC system [47]

Figure 11: Bonnet structure with shaker [47]

Duonian et al. [3] approximated the hood thickness to meet three targets HIC[24], mass and modality (Meeting the requirements of lightweight and reducing vibration and noise). To verify the reliability of their work, collision of pedestrian heads and hood was re-simulated. Noting that hood thickness is the most tractable part when it comes to hood optimization as the other parameters in geometry such as curvature must be consistent with the shape of the vehicle.

Hartley [50] proposed a method to predict the hyper-elastic[25] and dynamic behavior of an Ethylene Propylene Diene Monomer (EPDM) foam rubber. This material is widely used as a weather-strip component in car closures. It was observed that either static or dynamic response of the weather-strip material and component depends on factors such as excitation frequency, large-strain preload, vibration amplitude, geometry and also friction. A good correlation was observed between the experimental results and the proposed formulation for dynamic stiffness and loss factor below 100 Hz. Closure resonances predictions can significantly change based on the values assumed for weather-strip dynamic rate properties.

---

24 The Head Injury Criterion (HIC) is a measure of the likelihood of head injury arising from an impact. The HIC can be used to assess safety related to vehicles, personal protective gear, and sport equipment. Normally the variable is derived from the acceleration/time history of an accelerometer mounted at the center of gravity of a dummy's head, when the dummy is exposed to crash forces.

25 For many materials, linear elastic models do not accurately describe the observed material behavior. The most common example of this kind of material is rubber, whose stress-strain relationship can be defined as non-linearly elastic, isotropic, incompressible and generally independent of strain rate. Hyper elasticity provides a means of modeling the stress-strain behavior of such materials. The behavior of unfilled, vulcanized elastomers often conforms closely to the hyper elastic ideal. Filled elastomers and biological tissues are also often modeled via the hyper elastic idealization

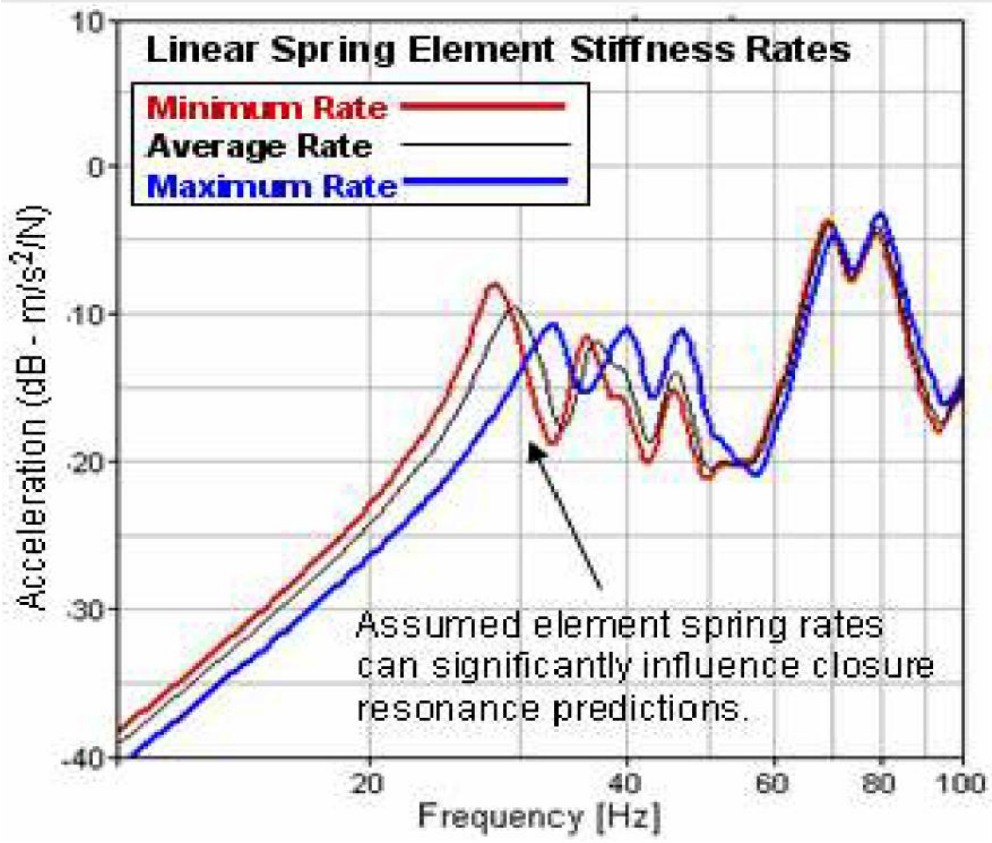

Figure 12: Effect of different dynamic rate assumptions on a door resonance [50]

2.3 Methods to improve vibrations and noise performance in Auto industry

The dynamic behavior of a component is a function of mass and its distribution, stiffness and damping. It can be modified in different ways such as adding layered damping materials, mass or changing geometry parameters, e.g., thickness [51].In car body panels, the following methods are used for damping vibrations energy [52].

The first method is made by attaching a viscoelastic layer with adhesive, spray or bond to the panel. This layer moves with the panel and dissipates vibrations energy to heat. Damping performance of this layer is a function of thickness, stiffness and the loss

factor. (extensional dampers). In addition, by adding a stiff layer like rubber, steel or foil to layers of viscoelastic material a new type of dampers which are called constrained layer dampers are created. When exposed to vibrations, the top constrained layer causes shear strain which forces the viscoelastic layers to remain fixed while the panel is deformed.

The thickness and stiffness of the top layer and loss factor of viscoelastic layer are effective in the damping behavior (constrained layer dampers). The friction of damping materials and also the friction between the layer and the panel in every cycle dissipate energy. Increasing the mass of the damper increases the friction dissipation. The contact between the viscoelastic material and the panel creates inelastic collision in each cycle, which can dissipate energy.

Qian et al. [52] studied different damping treatment behaviors for flat and geometrically stiffened panels. The damping treatments were characterized by reduction of average vibration amplitudes and FRFs. In practice, the stiffness of in-vehicle floor panels like tunnel, cross members and doorsills are not as high as clamped boundary conditions model but not as low as a panel with simply supported boundary conditions. Also they found that below 150 Hz, extensional dampers and constrained layer damper show similar effects on heavily ribbed panels. Constrained dampers have high damping performance above 150 Hz. Increasing the mass in sandwich type damper does not change the damping behavior significantly in frequencies between 150-250 Hz. Surface density increase in extensional dampers does not contribute to the damping performance in the low frequency range [52].

Tarnoczy [53] reported that smearing a damping layer on a steel panel can reduce the

radiated sound intensity by 10 dB and also a more effective noise reduction could be expected from a sandwich damper. The stiffness of front and rear bushings in vertical direction is the most effective parameters on the transmitted vibrations to the cabin [15].

Car panels in body structure are made of thin sheets of metal with very low bending stiffness. So increasing their stiffness is a common practice in industry [54]. By introducing curvature to the structure, low frequency modes are shifted to higher levels according to the equation below [54]:

$$f_{curved} = f_{flat} + \frac{1}{2\pi R}\sqrt{\frac{E}{\rho}} \tag{2.7}$$

Where, R is the radius of curvature and it works more effective than stiffening beads. Bending stiffness is proportional to the cross-section moment of area [55].

$$B = \frac{IE}{1-\nu^2} \tag{2.8}$$

Where, B is the bending stiffness, I is the moment of area of the cross section and ν is the Poisson's ratio. Low frequency noise improvement requires modification of vehicle structure [39]. First natural frequency of structure is the most important item to consider in system response [56]. The Effects of damping layers and stiffening ribs should be taken into account simultaneously [57].

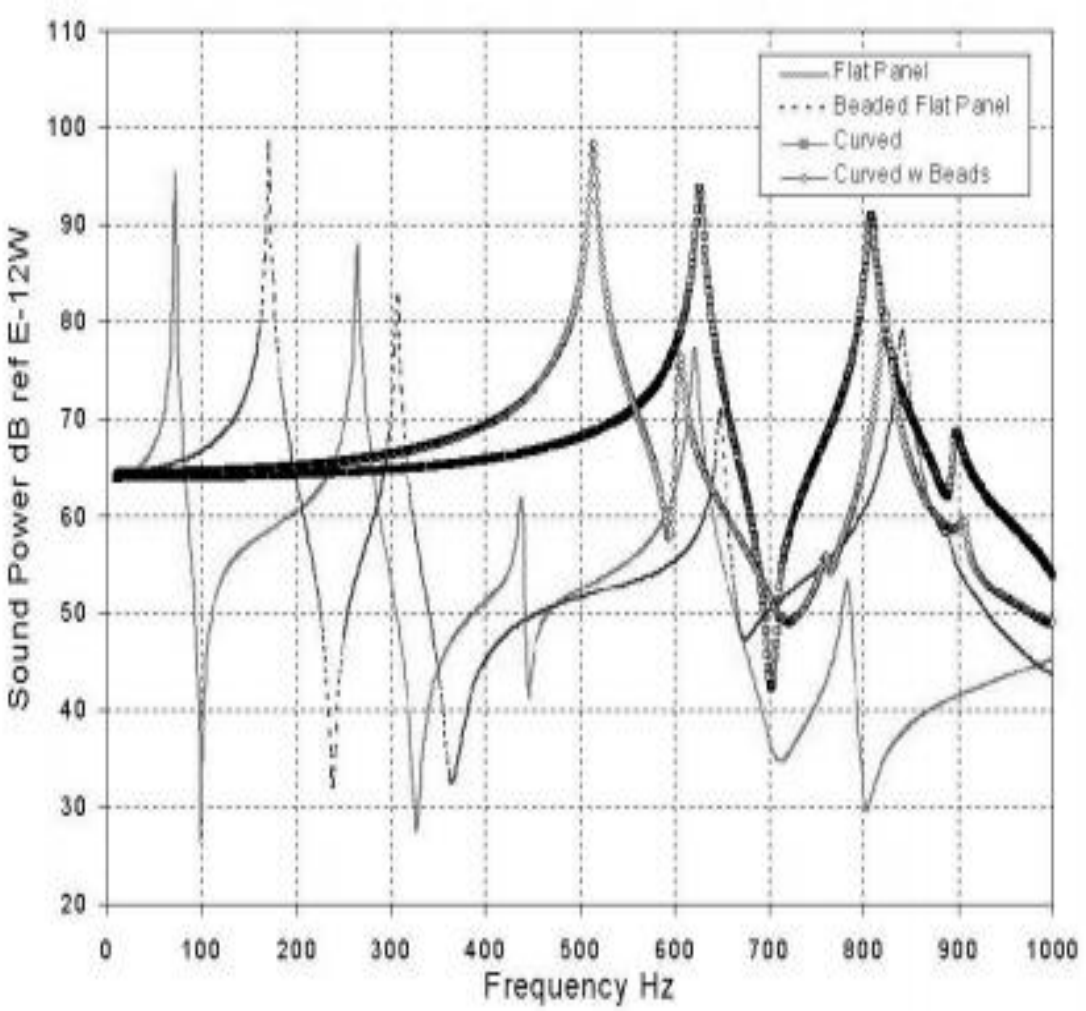

Figure 13: Effects of curvature on radiated sound power [54]

Introducing beads and ribs are common examples of geometric stiffening of a panel. They increase both the static and dynamic stiffness of the panel and shift the resonant frequency upwards. The interesting point is that the peak amplitude of the resonant frequency for a heavily ribbed panel is increased compared with the flat panel [52, 57]. for designing stiffening ribs, there are six design variables, namely, X and Y coordinates of the center of the ribs, location angle of the two ribs, length and width of the ribs [51].

Beads are features like channel which are added in metal forming process as an

inexpensive way to add stiffness to the panel to reduce noise and vibrations below 100 Hz. However, it must be noted that stiffening of a panel either by ribs or beads increases the radiation efficiency thus high frequency 1-5 KHz noise will increase [52, 54]. When it comes to thin plate structures, stiffening rib are an effective approach to reduce radiated noise. Cross ribs are adopted broadly to strengthen a plate [51]. Limited damping effects of extensional dampers on heavily ribbed panel were observed. While constrained layer dampers exhibited significant improvement in damping of these panels. As illustrated below, ribs can shift the frequencies but increase the amplitudes [53].

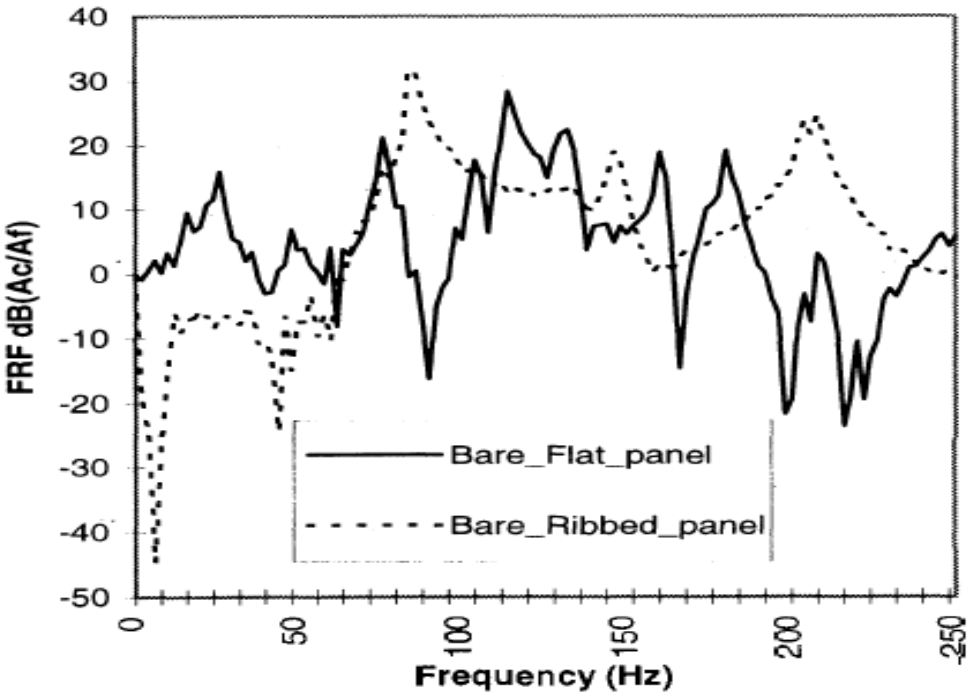

Figure 14: Influence of geometric stiffening [52]

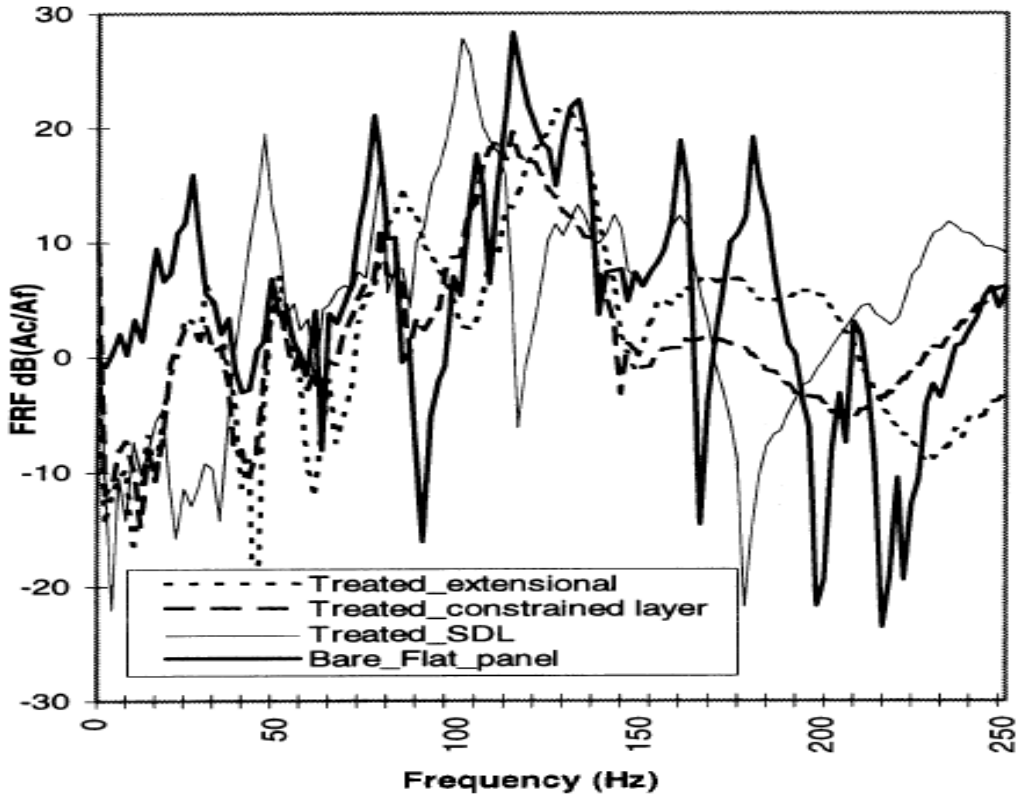

Figure 15: Performance comparisons of different dampers [52]

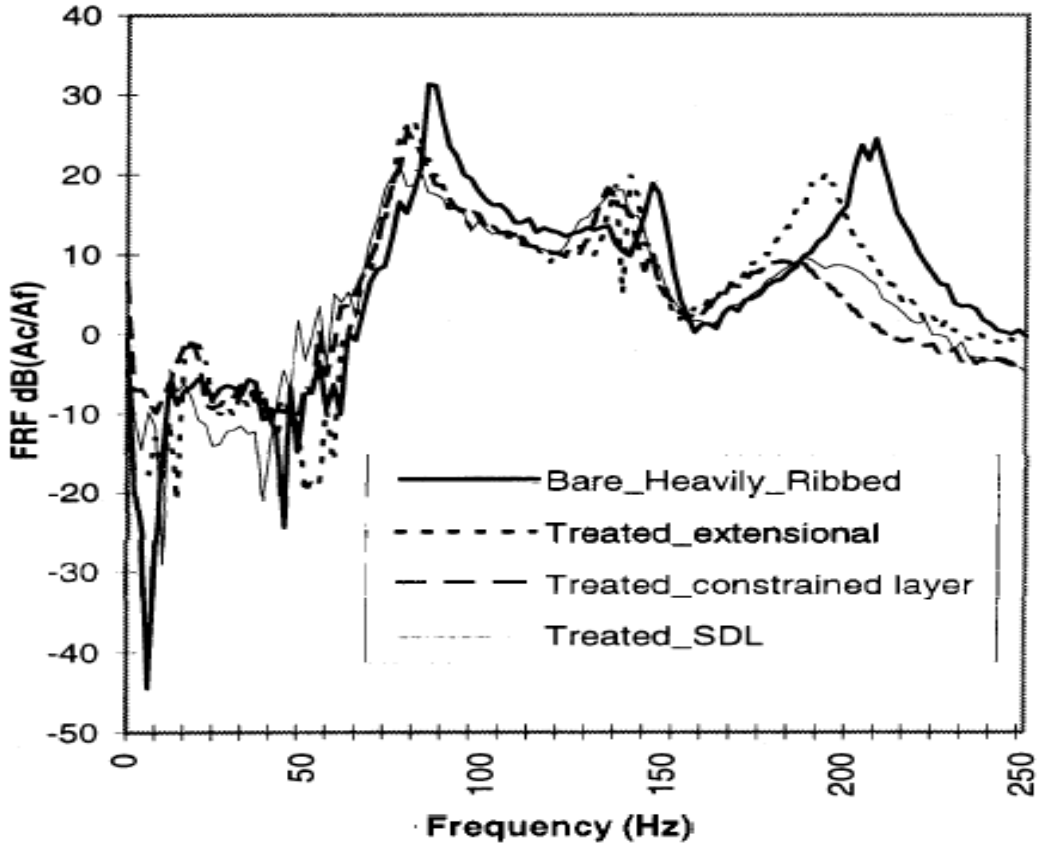

Figure 16: Performance comparison of different dampers applied on a heavily ribbed panel [52]

While stiffening beads can improve vibrations of first modes, they might increase the vibration levels on other frequencies. They can also increase radiation efficiency for a given frequency [55]. Pagnotta [56] utilized the Genetic Algorithm to find the optimum position and lay-out of stiffening ribs to shift the natural frequency of a car dashboard support. Similar to Pagnota's work, Carfagni et al. [57] proposed an approach based on CAE and Genetic Algorithm to achieve an optimal distribution of stiffening ribs and damping material. Their method reduced the damping material in the same vibrational performance.

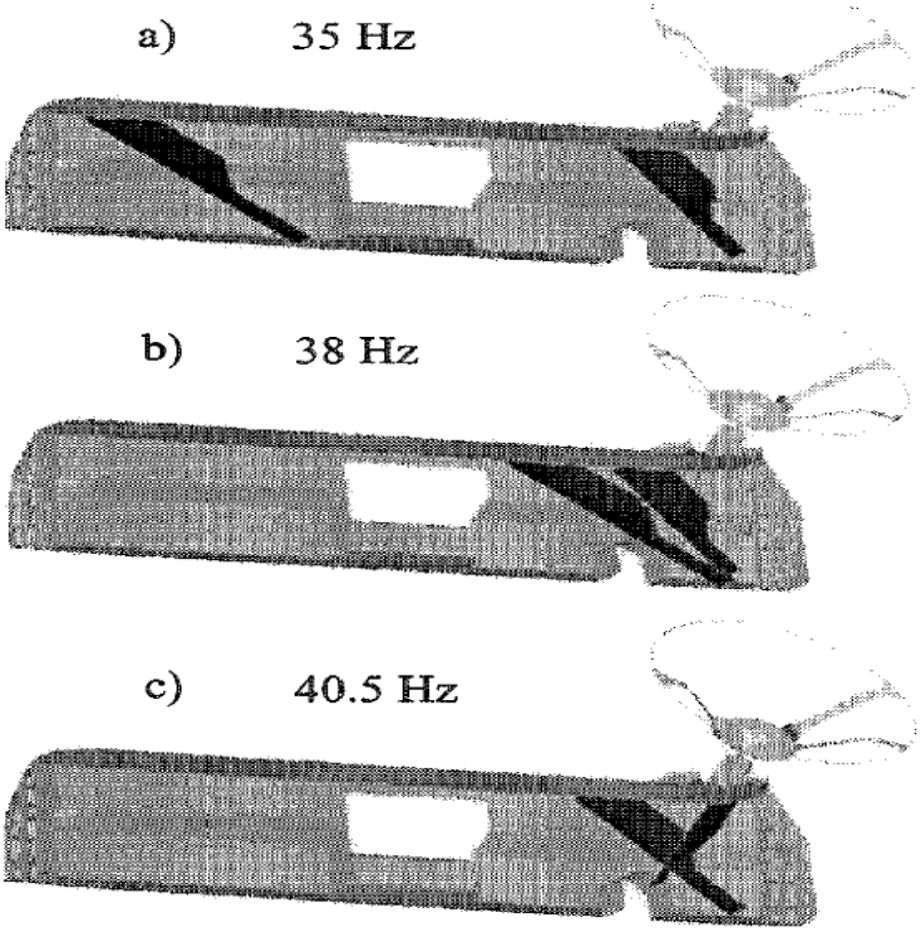

Figure 17: Effect of rib on stiffening of the panel [56]

Wind deflector is a feature installed on truck roof cabins to mitigate the drag force effect. Maladahiyar et al. [58] used Altair-Optistruct software to find the best configuration of the stiffening ribs. They validated the design with testing a prototype-built under dynamic loading conditions. Deng et al. [51] in 2005 found the best geometry and location of two cross stamped ribs in a plate to reduce resultant noise under wideband excitations.

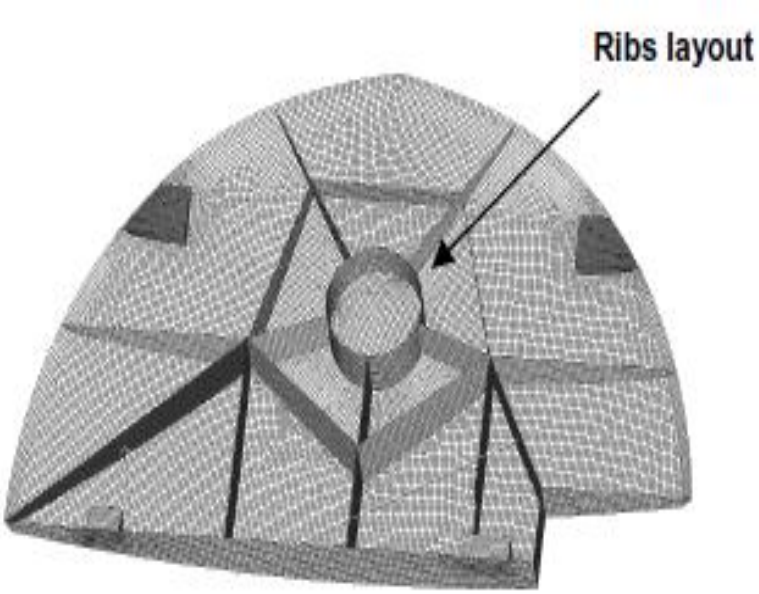

Figure 18: Optimized Rib Layout design on wind reflector [58]

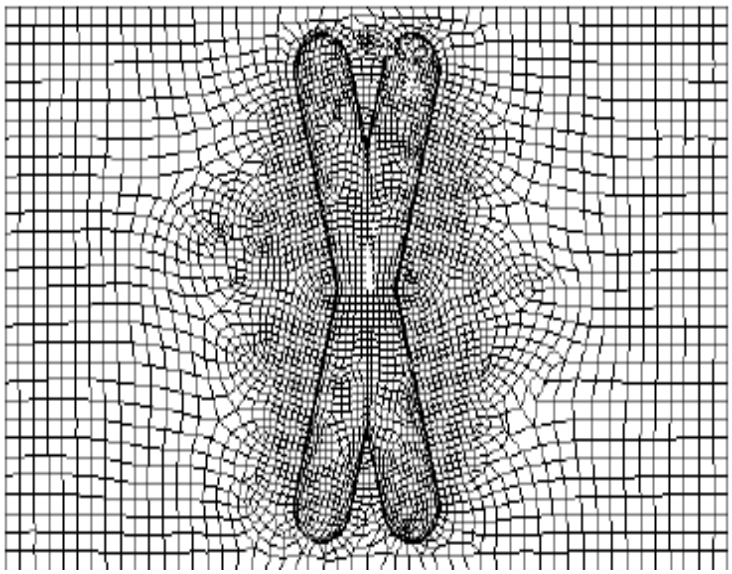

Figure 19: Optimal Cross ribs in the plate [51]

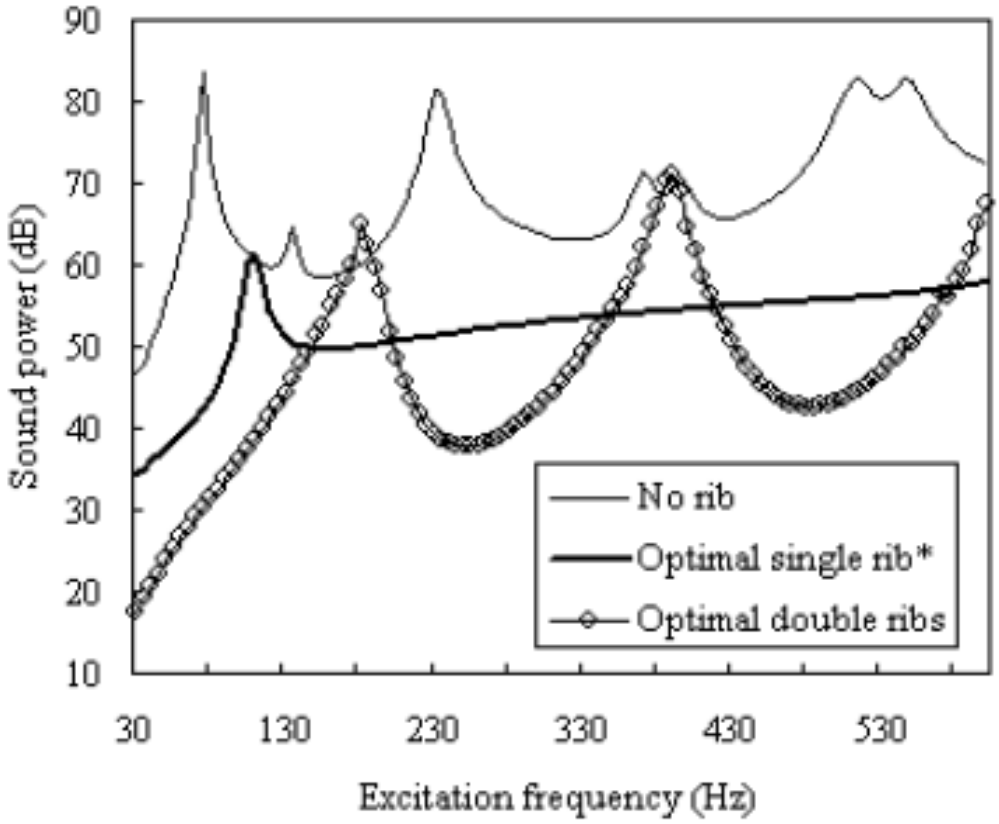

Figure 20: Variation of radiated sound power withe excitation frequency under three conditions; no rib, optimal single rib and Optimal double ribs [51]

Aydemir and Ebrinc [59] found an appropriate combination of increasing sheet thickness and rib to reduce noise emission of an intake manifold. A battery electric van, equipped with a developing permanent magnetic synchronous motor, exhibited annoying noises around. Through NVH data collecting and signal processing Lu and Jen [27] identified the cause of noise in a permanent magnetic synchronous motor. It was around 1.1 kHz and in 16th and 40th orders. When they sealed the cabin's leakage, a reduction of 4 dB interior noises and encapsulation of the motor led to a 6.5 dB noise reduction.

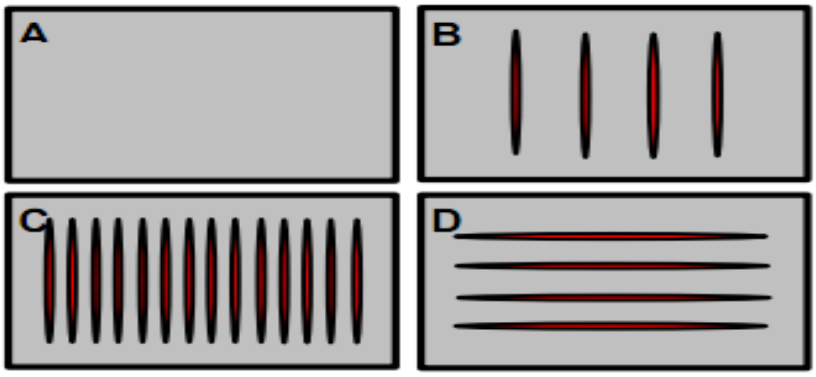

Figure 21: Basic Bead Configurations [54]

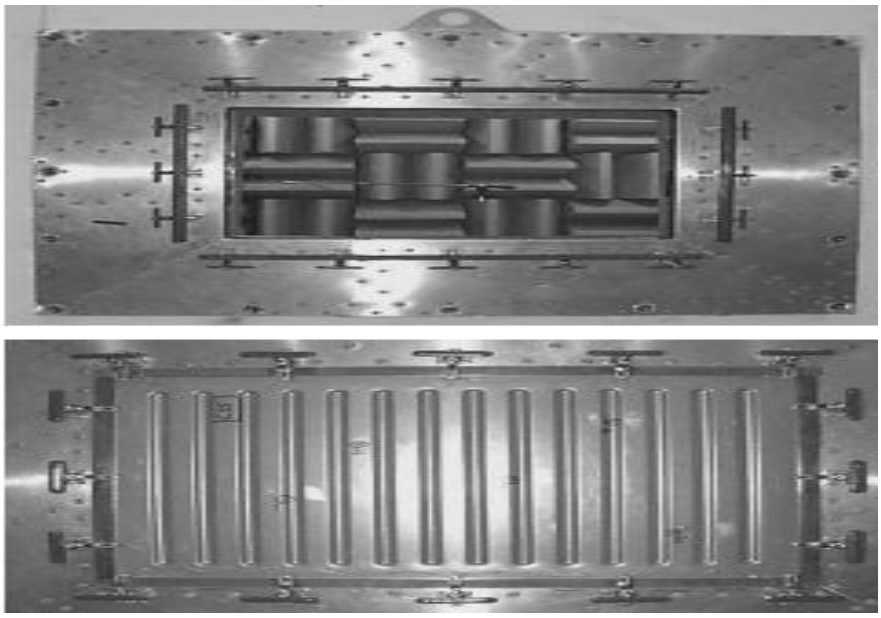

Figure 22: Bead-stiffened panels [54]

The interface components between front chassis and vehicle body like sub frames are important in reducing cabin road-induced vibrations and noise. Using ADAMS/CAR software, engine subframe parameters based on sensitivity analysis through Design-Of-Experiment[26] were optimized by Safaei et al. [15].

[26] In general usage, design of experiments (DOE) or experimental design is the design of any information-gathering exercises where variation is present, whether under the full control of the experimenter or not.

CHAPTER 3 DYNAMIC CHARACTERIZATION OF VEHICLE HOOD PANEL USING EMA AND CAE

As stated before, modal parameters which are gained by CAE are in need of validation. As not all the nonlinearities of elastic bumpers, bushing, hinges and latches can be modeled thoroughly in FEM. CAE output are normally validated with EMA or Optical field measurement. In this chapter, natural frequencies and mode shapes which are extracted by MSC Nastran software are correlated with EMA to validate the CAE model.

3.1 CAE Modal Analysis

FEM proves to be an essential tool to find mode shapes and natural frequencies of car component in earlier stages before manufacturing. Most in-vehicle and out-vehicle components are extensively analyzed under static and dynamic loads by FEM in development from conceptual design up to the final step. Natural frequencies, Frequency response functions, mode shapes and operational mode shapes of each component itself or in connection with others can be achieved by FEM under various conditions. A wide variety of commercial FEM codes have been developed and introduced to automotive industry so far. The whole process of an FEM analysis can be divided into pre-processing, processing and post-processing. Preprocessing, also called Meshing, is the first step in solving a problem in finite element analysis. In this step entire physique is divided into meaningful divisions often called "Elements". These elements form the building block on which the Boundary conditions and external effects are specified. Geometry used for meshing, can be imported from CAD [27]or be created in the FEM software. As most car

[27] Computer-Aided Design

components are very elaborate in physique, mostly a CAD model created in computer softwares like CATIA, UGNX, Solidworks, etc. the geometry is often imported into the FEM software. The after defining the appropriate analysis, one-dimensional, two or three, based on Element type, such as shell, solid, beam, etc. Meshing is started. Lastly boundary conditions, loadings and constraints are defined in this step. Altair Hypermesh is a common computer codes used in preprocessing.

Processing stage is like calculating and solving the equations to find the desired output. Based on the analysis type, linear static, modal, FRF, Fatigue, etc. commercial codes like Altair Radioss, MSc Nastran and Abaqus are widely used for this purpose.

The obtained results can be seen and analyzed through post-processing softwares like Altair Hypergraph, Altair Hyperview and etc. In this study, Altair Hypermesh, MSc Nastran, Altair Hyperview and Altair Hypergraph are employed to extract modes shapes and natural frequencies of the panel.

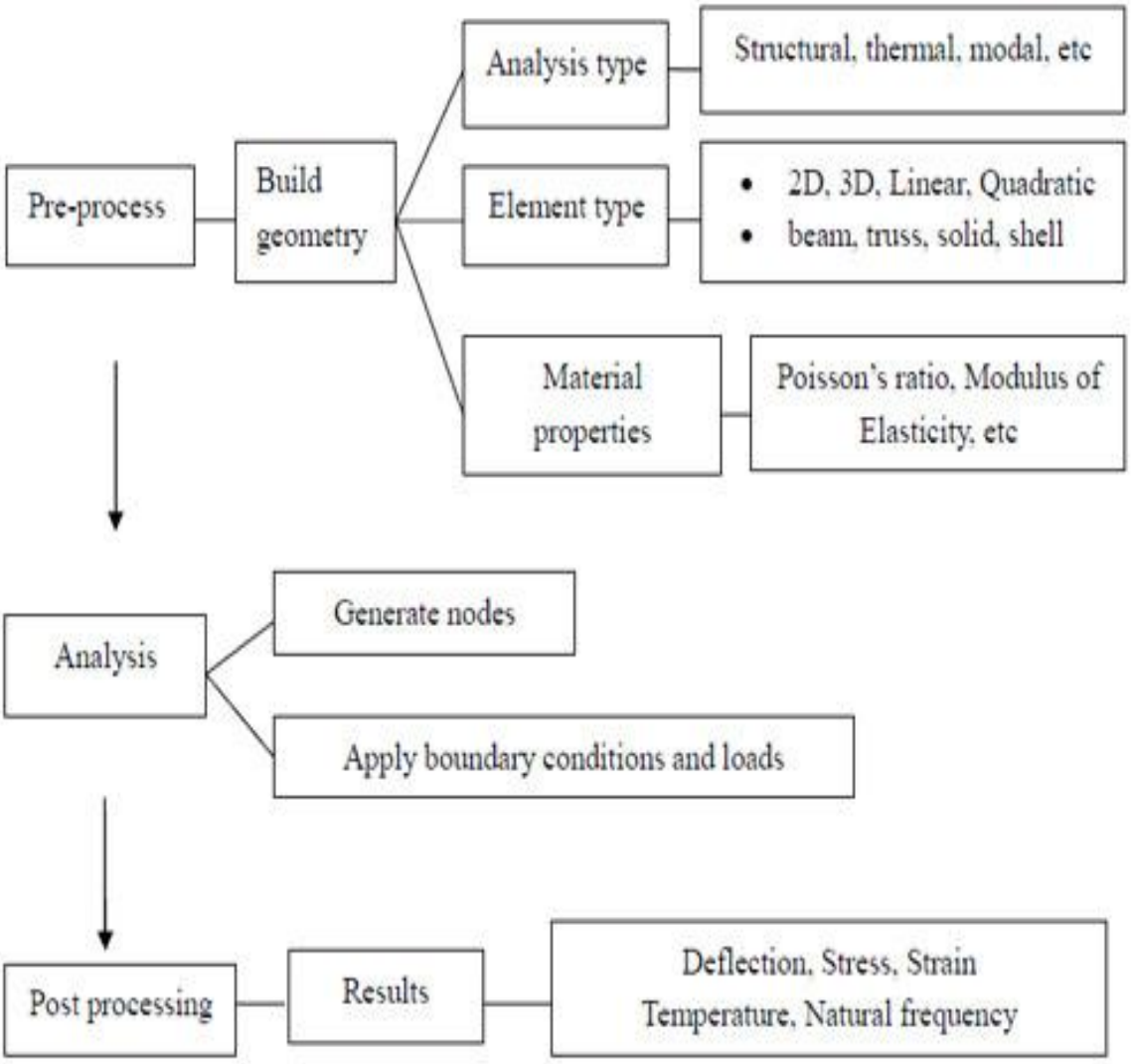

Figure 23: FEM procedures for solving a problem [60]

3.1.1 Background of Eigenvalue Analysis in FEM

In finding natural frequencies and mode shapes of the component, damping effects are disregarded. This step is essential in product development as it gives clear understanding of the response of the component to loadings. To avoid massive vibrations, design must be in the way that the frequency of a dynamic loading does not match with the natural frequencies of the structure. Normal modes are also required to find the best

location of installing pick-ups. At every frequency the structure is deformed in a particular pattern which is called a mode shape. Mode shapes and natural frequencies depend on the components properties like elasticity modulus, dimensions and cross sections and also boundary conditions[45].

Mode shapes and natural frequencies are obtained by solving an eigenvalue problem. Eigen values are natural frequencies and eigenvectors are the associated mode shapes. Without damping and loadings, matrix format of the equation of motion is [61]:

$$[M]\{\ddot{u}\} + [K][u] = 0 \quad (3.1)$$

where, M denotes inertia matrix, $\ddot{u}$ is acceleration, K is stiffness and u is displacement. Like classic methods of solving vibrations problems, a harmonic solution is assumed for the above mentioned formula.

$$\{u\} = \{\varphi\} sin\omega t \quad (3.2)$$

$\{\varphi\}$ is the eigenvector and ω is the natural frequency.

Harmonic solution assumption leads to the fact that all particles of the components move simultaneously so the basic shape remains unchanged and only the amplitudes fluctuate.

Substituting the second equation into the first one result in the Eigen equation as:

$$([K] - \omega^2[M])\{\varphi\} = 0 \quad (3.3)$$

Based on linear matrix algebra; eigenvalue problem is in the form of;

$$[A - \lambda I]x = 0 \quad (3.4)$$

A is a square matrix, λ is eigenvalues, I is the identity matrix and x is eigenvector.

Comparing the third and the second equations, $\lambda = \omega^2$

So equaling determinant of $([K]-\omega^2[M])\{\varphi\}$ to zero, gives the eigenvalues which determine a mode shape.

And eigenvectors are:

$$([K]-\omega^2[M])\{\varphi_i\}=0, \tag{3.5}$$

i=1,2,3,4,..

Deflected shapes of a linear elastic structure at any time can be found with superposition of product of mode shapes and modal displacement;

$$\{u\}=\sum_i(\varphi_i)\xi_i \tag{3.6}$$

In order to check that each normal mode is distinct from the other, orthogonally of normal modes is introduced;

$$\omega_j^2=\frac{\{\varphi_j\}^T[K]\{\varphi_j\}}{\{\varphi_j\}^T[M]\{\varphi_j\}} \tag{3.7}$$

$$\{\varphi_i\}^T[M]\{\varphi_j\}=\begin{cases}0\ for\ i\neq j\\1\ \ for\ i=j\end{cases} \tag{3.8}$$

Different methods are solving numerical equations leads to various computational methods to extract real eigenvalue extraction are applied in CAE dynamic analysis solvers. All the methods work for all the problems but none of them is best for all problems. These methods are derived from either transformation or tracking method. In the first method, the eigenvalue equation is transformed to a special form to get eigenvalues in a straightforward way. In second approach, Eigenvalues are derived on an iterative procedure to derive one at each step. MSC Nastran [61] recommends Lanczos method for real eigenvalue extraction which is a convenient fusion of both transformation and tracking methods. Givens method, Modified Givens method, Householder method and

Modified Householder method are available methods based on transformation methods. Real eigenvalue extraction methods based on the tracking are Inverse power method and Sturm modified inverse power method. Bulk data of EIGRL and EIGR define Lanczos method all of the other methods respectively and SOL 103 is the unique denotes normal modes extraction in MSC Nastran.

3.1.2 Hood panel construction

A typical hood is shown in Figure 23. The geometry of a typical hood consists of the top panel, inner panel, hinges, latches and elastic bumpers. Two latches on the two corners of the top part retain the structure and attach it to the body. One or two hinges on the front most of the components lock the structure in front. Normally hinges and latches are made of steel while the sheet panels are aluminum alloys [1, 2].

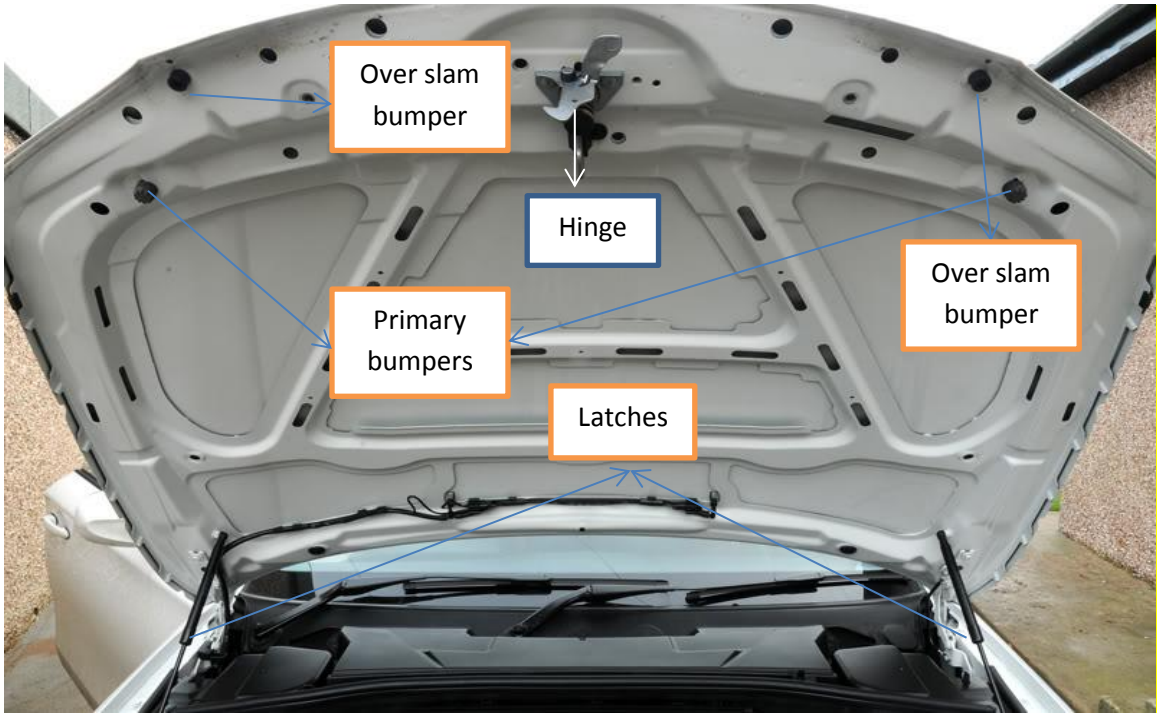

Figure 24: Geometry of a typical hood (Honda Accord, 2014)

3.1.3 Boundary conditions of the FEA

Primarily there are three constraint locations. They are hinges, latches and elastic bumpers. Bumpers are small flexible objects which are widely used in order to facilitate matching the body and hood and also to provide compliance against mechanical stresses. Bumpers are usually modeled as a spring with defined stiffness in three directions. The ends of these springs on the body are constrained in all directions [1, 2].

Based on the previous works on CAE of hood panel, all degrees of freedom in translational X,Y,Z and rotational X,Y and Z are constraint for hinges [1, 2]. Panels are meshed with four-node quadrilateral shell elements.

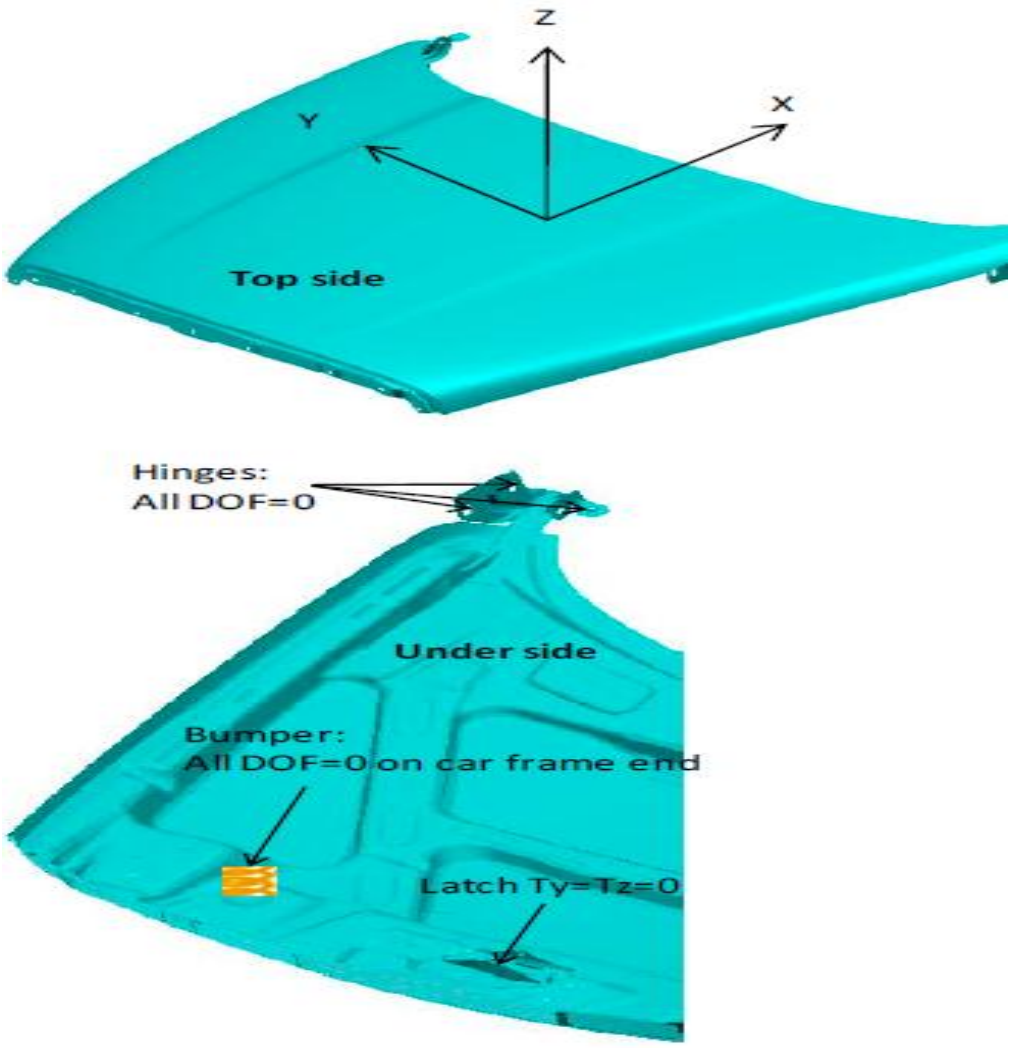

Figure 25: Hood panel model used by Gupta [2]

According to Gupta [2], the first mode at 20.5 Hz they found is a torsional mode. The second one was oil canning[28] at 22.2 Hz and bending because of Y rotation allowance in their model. The third mode at 26.4 Hz was similar to the second toward negative Y direction.

[28] Oil canning is defined as a visible waviness in a flat areas of metal surface (Metal construction association, Technical bulletin)

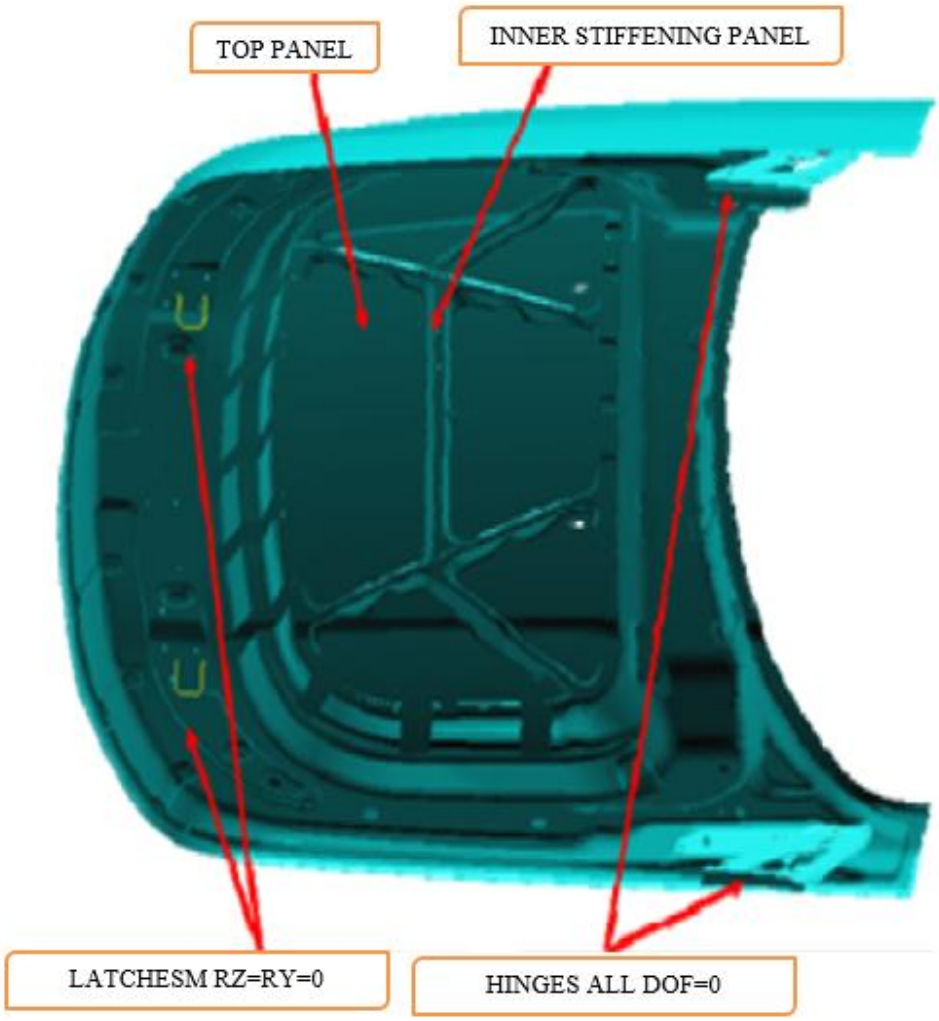

Figure 26: Hood panel model used by Gaylard [1].

Gaylard [1] found that in their model, the oil canning happens at 23.9Hz and in the first mode, the first torsional mode is at 26.3 Hz and third mode at 31.3 Hz is also torsional. There are some similarities between first and forth mode at 33.8 Hz with difference of inward Y direction oil canning.

In any case the first few modes are most important regarding dynamic deformation. So any periodical force in this range will result in course vibrations. Hanouf et al. [45] found that the first mode of his CAE model of a hood panel occurs at 53.05 Hz in a simple

bending mode. The second one which is torsional is at 58.83 Hz. Second bending mode happened at 76.08 Hz with low oscillation amplitude. The second torsional mode was at 84.15 Hz with higher amplitude compared with the third mode.

3.1.4 Evaluation of the structural resonance frequencies

Based on two criteria for constraining latches, the CAE model is run to extract natural frequencies of the hood panel. The resultant first ten natural frequencies of the hood panel are listed in table 2.1. The first mode exhibits oil-canning at around 24 Hz. The bending happens around z axis. The first torsional mode happens at 45.6 Hz. third mode is very similar to the first mode at 66.9 Hz but with less oscillation amplitude. Forth mode is a torsional one affecting the lower part of the panel rather the top part. Expectedly, the fifth mode at 90.03 Hz is bending focusing at upper area. The sixth mode is again bending which only concentrates at lower parts.

Table 3.1: CAE mode extraction

	Latches constraint in translational Y and Z	**Latches constraint in rotational Y and Z**
First Mode	24.3 Hz	24.17 Hz
Second Mode	45.6 Hz	45.51 Hz
Third Mode	66.91 Hz	69.38 Hz
Forth Mode	81.66 Hz	76.4 Hz
Fifth Mode	90.03 Hz	90.9 Hz
Sixth mode	103 Hz	101.3 Hz

3.2 Experimental Modal Analysis

Experimental Modal Analysis is a method to obtain dynamic characteristics of a structure in terms of its modal parameters; Natural frequencies, Damping and modes shapes. Practically, EMA consists of three steps [62] :

1- Measurement of FRFs

2- Estimation of Modal Parameter

3- Validation of the mode shapes

Generally Frequency Response Function of any dynamic system can be obtained in 3 steps:

1- Writing equation of motions in time domain

$$[M]\{\ddot{X}\} + [C]\{\dot{X}\}+[K]\{X\} = f(t) \quad (3.9)$$

Where, $[M]$, $[C]$ and $[K]$ indicate mass, damping and stiffness matrix and f denotes the external force in time domain.

2- Fourier transform to have the equation in frequency domain

$$(-M\omega^2 + j\omega C + K)X(\omega) = F(\omega) \quad (3.10)$$

3- Finding FRF as a fraction of output to input of the system

$$X(\omega) = H(\omega)F(\omega) \quad (3.11)$$

$$H(\omega)=[-\omega^2 M + j\omega C + K]^{-1} \quad (3.12)$$

Where, $H(\omega)$ is the transfer function between input and the output of the system.

This equitation can be also expressed in the following format:

$$H(\omega) = \sum_{r=1}^{n} \frac{(\varphi_i \varphi_k)_r}{[\omega_r^2 - \omega^2 + 2j\xi_r\omega_r\omega]} \quad (3.13)$$

Modal parameters can be obtained with one complete row or column of FRF matrix

$$H = \begin{bmatrix} H_{11} & H_{12} & H_{13} & H_{14} \\ H_{21} & H_{22} & H_{23} & H_{24} \\ H_{31} & H_{32} & H_{33} & H_{34} \\ H_{41} & H_{42} & H_{43} & H_{44} \end{bmatrix} \quad (3.14)$$

In the matrix above, Columns indicate inputs and rows are for responses. Because of the reciprocity $H_{mn} = H_{nm}$ and also H_{mn} is the response at m due to excitation at n.

3.2.1 Equipment for measurement of FRF

Excitation or input of the system can be Shakers, mostly in laboratories and impact hammers which are extensively used in industry. Impact hammers have a force sensor in the head. It measures the amplitude and frequency content of the energy transferred to the structure. They are used in modal analysis, resonance testing and also structural health monitoring.

Figure 27: Impact hammer[63]

Measuring devices are mostly vibrations pick-ups like piezoelectric accelerometers made by PCB. Two types of them are widely used in industry. The one with built-in signal conditioning electronics which are called ICP and the second types are without this option. Because of the convenience in use, easier set up and appropriate cost ICP types are more preferable unless in high temperature which may harm the electronics components in ICPs [63].

In another class, accelerometers are triaxial or uniaxial. Triaxial accelerometers

measure vibrations in all three directions. So each axis has an independent channel for data acquisition system. Expectedly, this type of accelerometers is very popular because of the convenience they offer in exhaustive measurement of structure dynamic behavior [63].

Figure 28: Triaxial accelorometer [63]

Measurement System consists of FFT analyzer, Data acquisition, Front end and PC. Modern and more sophisticated systems offer a package including software and hardware to obtain signal, processing and giving the desired output in a desirable format.

3.2.2 Experimental Modal Analysis of the Hood Panel

The hood geometry created in LMS software package is illustrated in Figure 30. As can be seen, Entire surface of the structure is divided into 9 points. Only five accelerometers are used so different iterations are applied. Driving points are at 5, 6, 9 and two points at each iteration are impacted by the hammer. The first iteration is run with points 5,6,7,8 and 9.

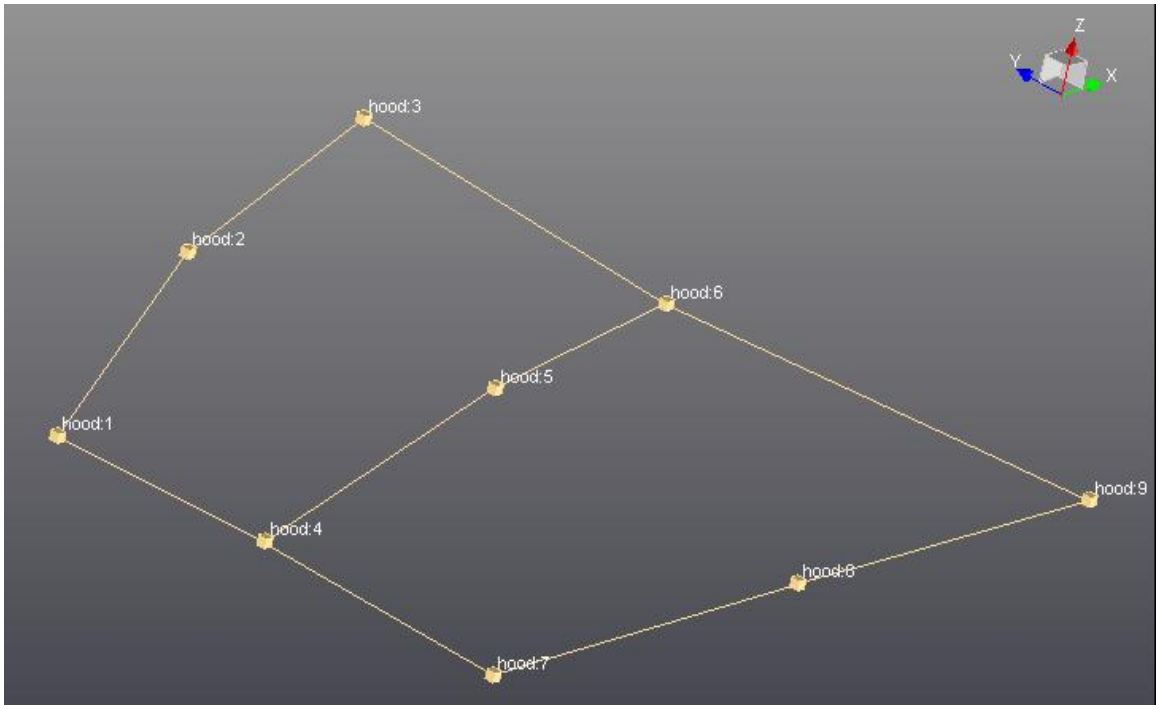

Figure 29: Geometry created in LMS

In the second run points 1,2,3,4 and 5 are included. Intentionally, Point 5 is kept unchanged in this practice to be considered as a reference point. Washers of same weight as the accelerometers are used in each iteration for not shifting frequencies due to change in mass. After obtaining FRFs of all points, Curve fitting on stabilization diagram will give the mode shapes.

Based on Least Square Complex Exponential Method (LSCE)

$$H(\omega) = \sum_{k=1}^{n} \frac{A_k}{j\omega - \lambda_k} + \frac{A_k^*}{j\omega - \lambda_k^*} \quad (3.15)$$

$$A_k = Q_K\{\varphi_K\}\langle\varphi_K{}^T\rangle \quad (3.16)$$

$$\lambda_k , \lambda_k^* = \xi_k\omega_k \pm j\omega_k\sqrt{1-\xi^2_k} \quad (3.17)$$

Q_K is the modal scaling factors and$\{\varphi_K\}$ is mode shapes.

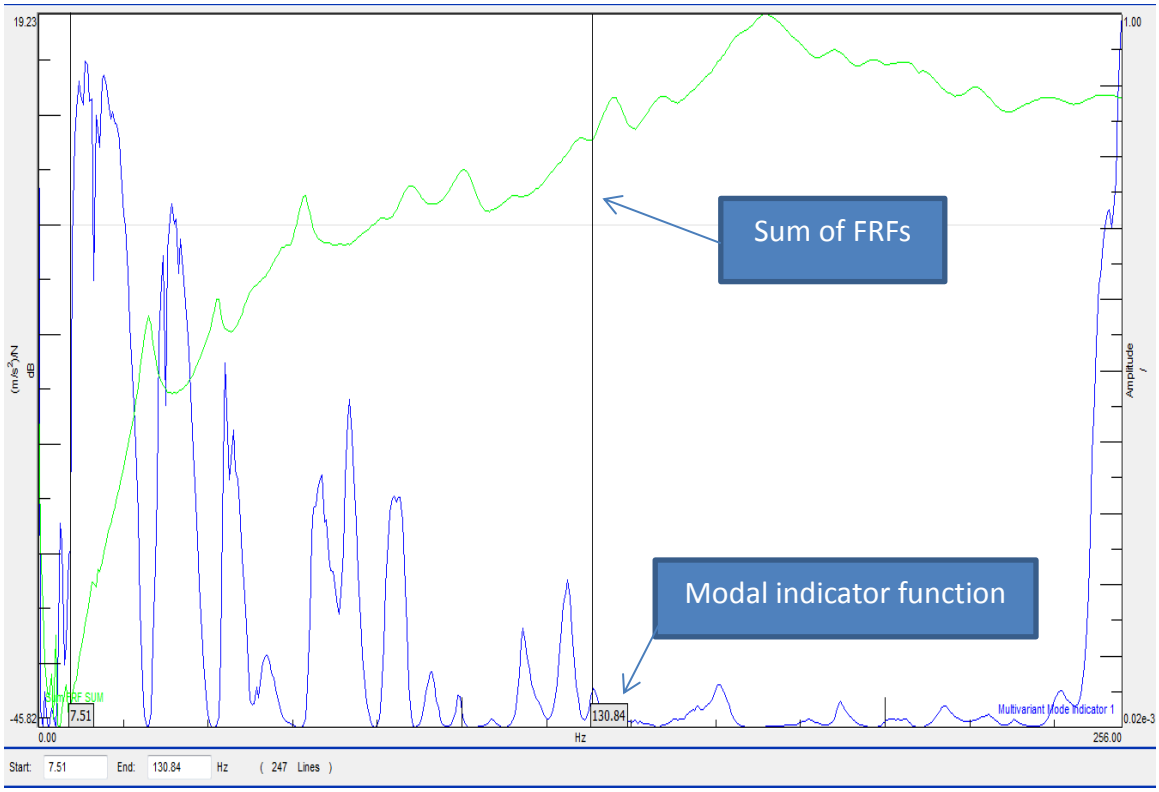

Figure 30: Modal analysis

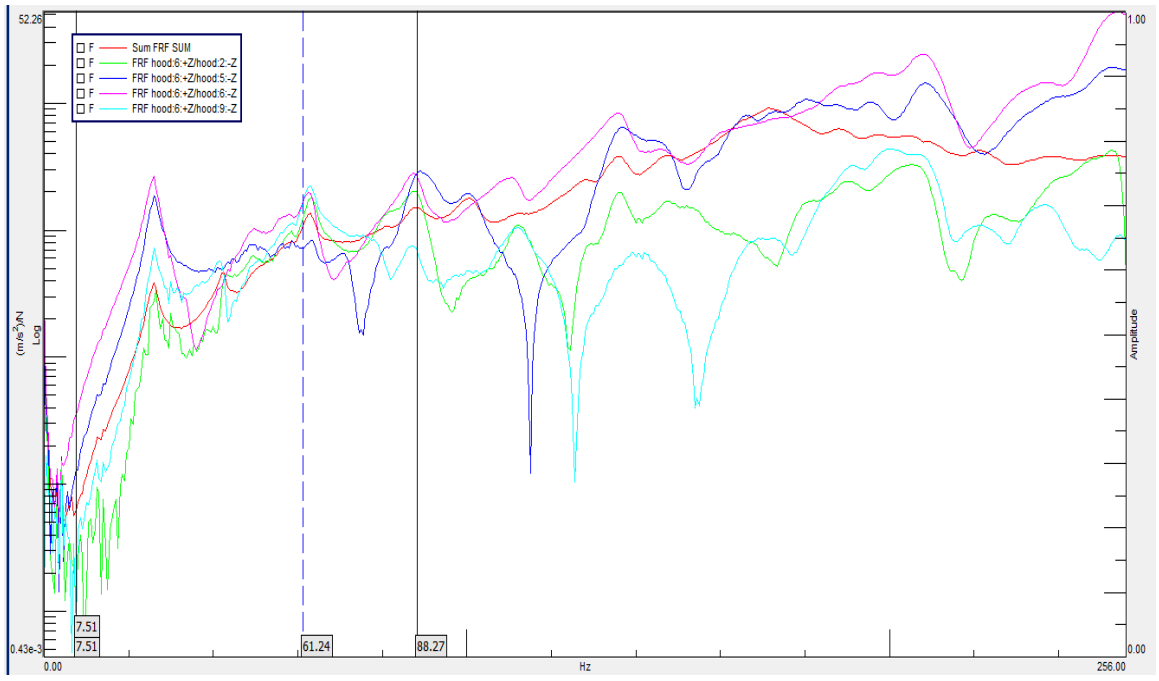

Figure 31: FRF demonstration

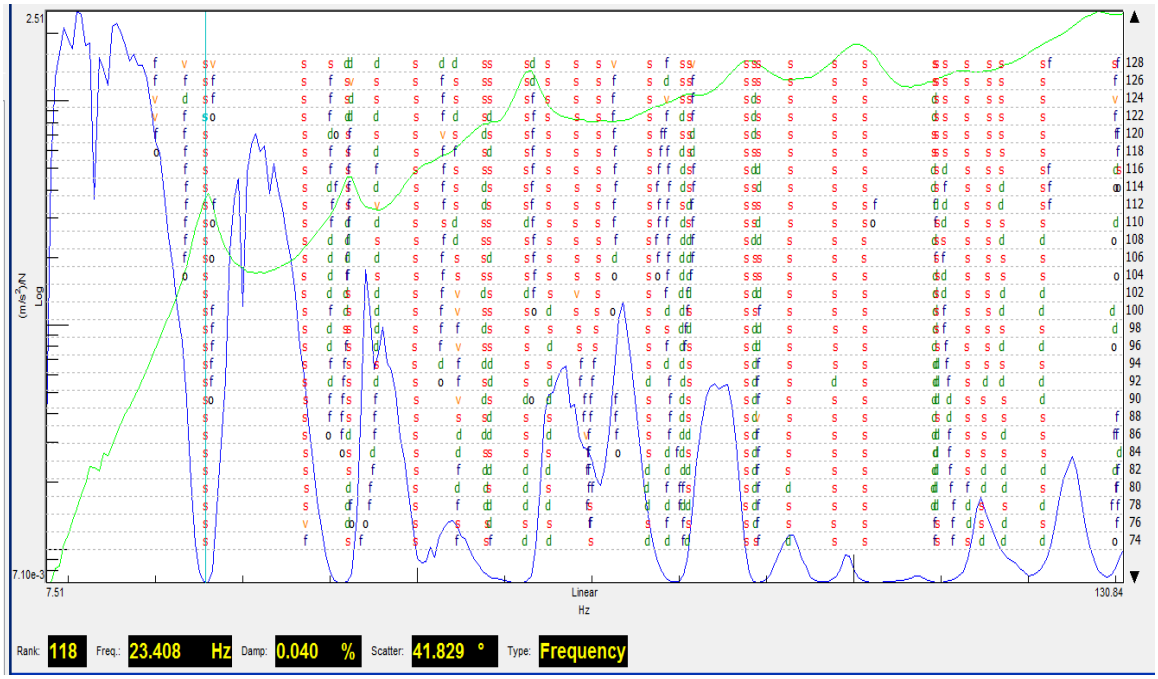

Figure 32: Determination of mode shape and curve fitting

Table 3.2: Modal parameters from EMA

Mode index	Resonance Frequency	Damping
Mode 1	25.7 Hz	3.35 %
Mode 2	42.15 Hz	1.93 %
Mode 3	62.51 Hz	2.97%
Mode 4	80.313 Hz	2.15 %
Mode 5	87.79 Hz	3.74 %
Mode 6	101.25 Hz	3.35 %

The mode shapes are correlated closely with the ones obtained by CAE. FEM is expected to give higher frequency rather than experiment; apart from the first resonance

this work confirms their study [47]. Furthermore, No significant difference were observed in most frequencies between constraining Y and Z rotational or translational motion. Comparing mode shapes of EMA and CAE is necessary to find the related frequencies, as the solver sometimes gives fake modes. Due to not considering non-linearities as it is in reality. Finally, the results from CAE are found clean and clear. These results contained natural frequencies and their corresponding modes shapes. Correlation of these values with experiment is one of the objectives of this work.

Table 3.3: CAE and EMA correlation

	EMA	**Latches constraint in translational Y and Z**	**Deviation from EMA In percent**	**Latches constraint in Rotational Y and Z**	**Deviation from EMA In percent**
First Mode	25.73 Hz	24.3 Hz	5.6	24.17 Hz	6.1
Second Mode	42.15 Hz	45.6 Hz	-8.2	45.51 Hz	-8.0
Third Mode	62.52 Hz	66.91 Hz	-7.0	69.38 Hz	-11.0
Forth Mode	80.31 Hz	81.66 Hz	-1.7	76.4 Hz	4.9
Fifth Mode	87.8 Hz	90.03 Hz	-2.5	90.9 Hz	-3.5
Sixth mode	101.25 Hz	103 Hz	-1.7	101.3 Hz	0.0

CHAPTER 4 RANDOM VIBRATIONS ANALYSIS VIA CAE

Random oscillations are complicated to analyze due to inherent nonlinearities and unpredictability nature. Therefore, extensive uses of CAE methods are inevitable to have the most accurate estimation of a system response under random inputs. Earthquake, airplane wings flutter under aeroelasticity excitations and road base excitation due to its unevenness are common examples of using random vibrations analysis. In chapter one, random nature of road irregularities and related equations were reviewed. In this chapter, the method which is used by MSC Nastran to find response of a system under random excitations will be addressed. Then the method to find inputs of the system and finally the response of the system will be stated **[61]**.

4.1 Random vibrations analysis in MSC Nastran

Random response analysis in MSC Nastran is based on data reduction[29] to frequency response analysis. Entire Procedure can be classified in three steps[61]:

1- Executing frequency response analysis for a sinusoidal loading conditions, $\{P_a\}$ in each loading condition (a) and a sequence of frequencies ω_i

2- Applying data reduction to the findings of step 1 to find $u_{ja}(\omega_i)$ as the output

3- Calculation of PSD and autocorrelation functions for the outputs from 2

Thus if autocorrelation of loading a, is denoted by S_a and cross spectral density of loading a and b areS_{ab}, frequency response $H_{ja}(\omega_i)$ then response quantity is S_j. In the

[29] **Data reduction** is the transformation of numerical or alphabetical digital information derived empirically or experimentally into a corrected, ordered, and simplified form. The basic concept is the reduction of multitudinous amounts of data down to the meaningful parts.

last step PSD of the response in displacement, velocity or acceleration is calculated according to the flow diagram illustrated in Figure 33.

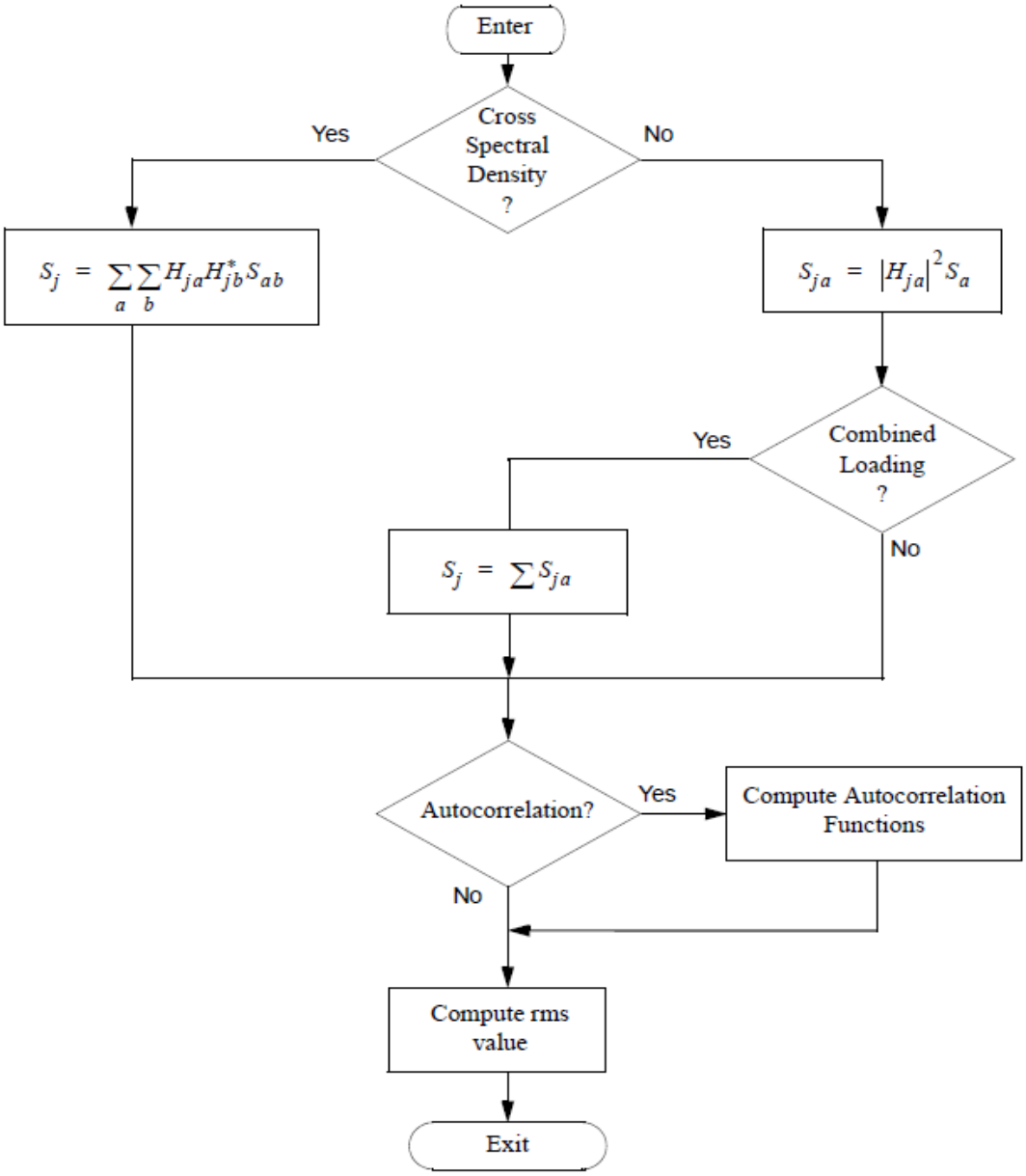

Figure 33: Flow diagram for Random Analysis module[61]

Random process analysis based on frequency response techniques requires that [61]

1- Linear system

2- Time stationary excitations

Autocorrelation function of a variable u_j is

$$R_j(\tau)=\lim_{T\to\infty}\frac{1}{T}\int_0^T u_j(t)\,u_j(t-\tau)dt \quad (4.1)$$

One sided power spectral density is

$$S_j(\omega)=\lim_{T\to\infty}\frac{2}{T}\left|\int_0^T e^{-i\omega t}\,u_j(t)dt\right|^2 \quad (4.2)$$

Autocorrelation function from frequency response function is :

$$R_j(\tau)=\frac{1}{2\pi}\int_0^\infty S_j(\omega)\cos(\omega\tau)\,d\omega \quad (4.3)$$

Root Mean Squared magnitude

$$\overline{u_j}^2=R_j(0)=\frac{1}{2\pi}\int_0^\infty S_j(\omega)\,d\omega \quad (4.4)$$

If the excitation source is Q_a, frequency response of a variable u_j is H_{ja} then

$$u_j(\omega)=H_{ja}(\omega)\,Q_a(\omega) \quad (4.5)$$

PSD of response, $S_j(\omega)$ is found based on PSD of source, $S_a(\omega)$

$$S_j(\omega)=\left|H_{ja}(\omega)\right|^2 S_a(\omega) \quad (4.6)$$

The last equation is important in evaluation of random response of a system by frequency response method. If sources are correlated;

$$S_j=\sum_a\sum_b H_{ja}H_{jb}^{*}\,S_{ab} \quad (4.7)$$

Cross-correlation function of two quantities is defined:

$$R_{ab}(\tau)=\lim_{T\to\infty}\frac{1}{T}\int_0^T u_a(t)\,u_b(t-\tau)dt \quad (4.8)$$

u_a And u_b can be displacement, velocity or single point constraint force response at a point.

Cross power spectral density, cross-PSD, of u_a and u_b are:

$$S_{ab}(\omega) = 2\int_{-\infty}^{+\infty} R_{ab}(\tau)\, e^{-i\omega t} d\tau \tag{4.9}$$

4.2 Finding random excitations coming from road irregularities

In order to describe random characteristics of the base excitations it was assumed that the inputs to the system come from the spots attaching the hood to the body.

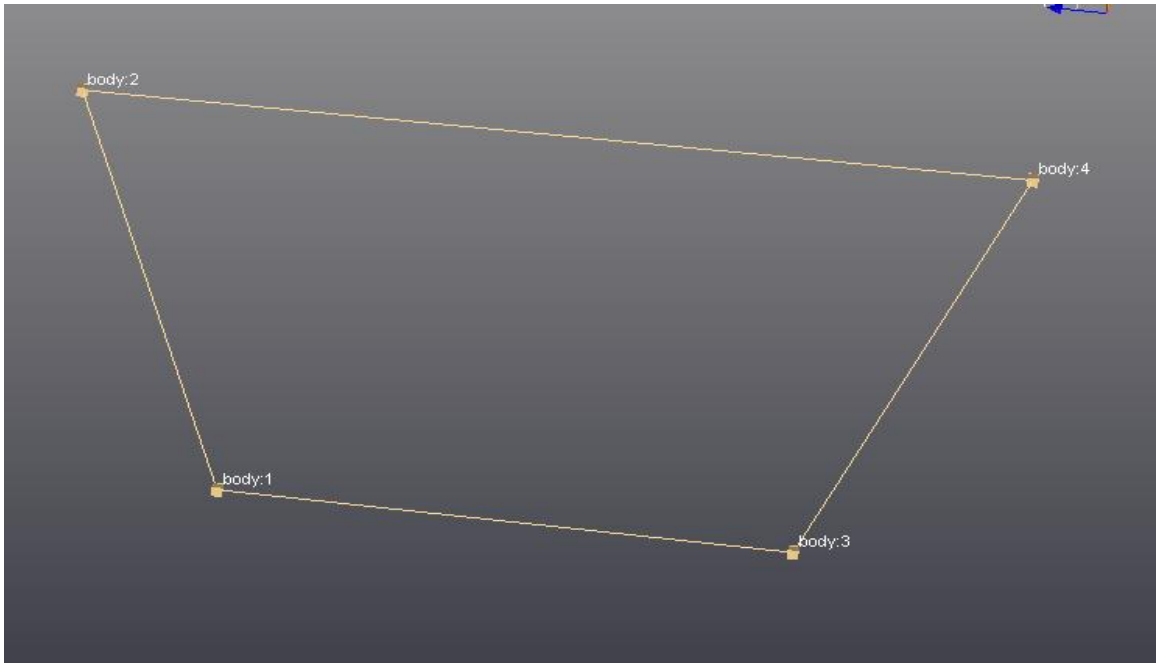

Figure 34: Four body points to receive random base excitations

Rough road as a typical road conditions is considered. According to the literature review, in order to be able to consider the process as stationary a constant velocity must be followed. Either 30 -40 MPH sound reasonable for this approach. PSD vs frequency trends are obtained for the for body points.

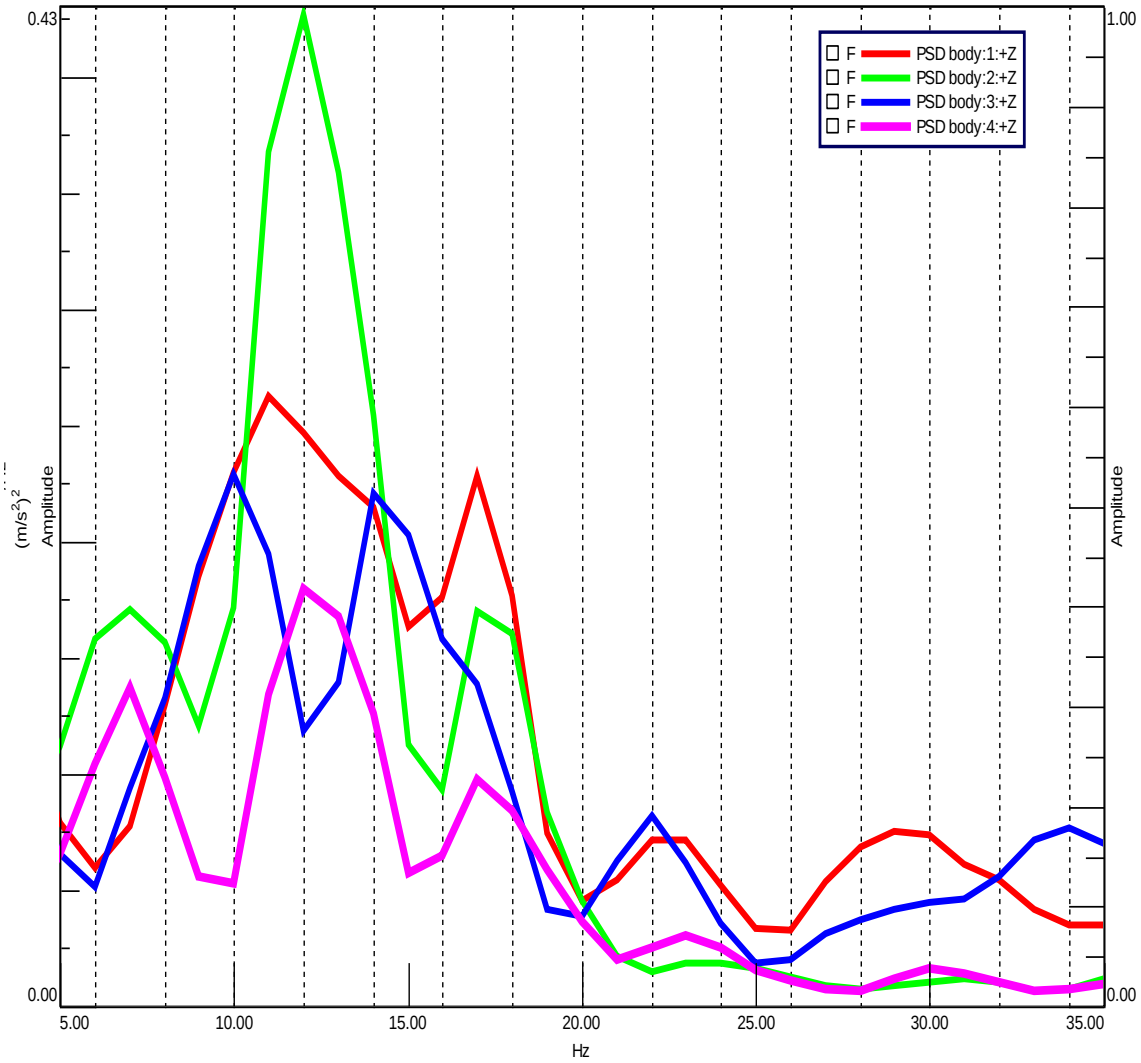

Figure 35: PSD vs Frequency trend for 4 body points

In order to see how each excitation points influence the others cross PSDs must be considered also. These values are extracted in real and imaginary vs frequency trend.

The findings are as follow:

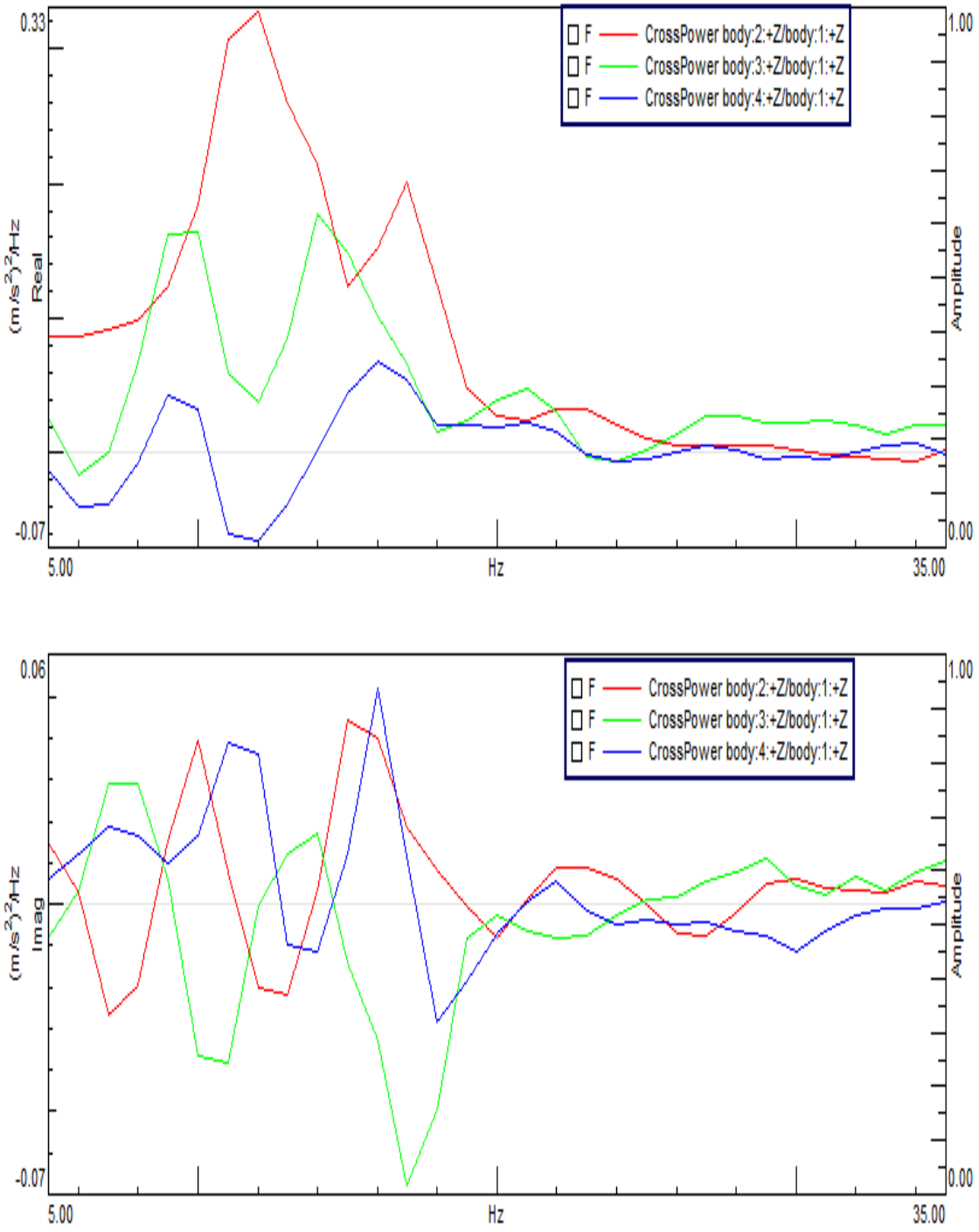

Figure 36: Cross PSD about point one

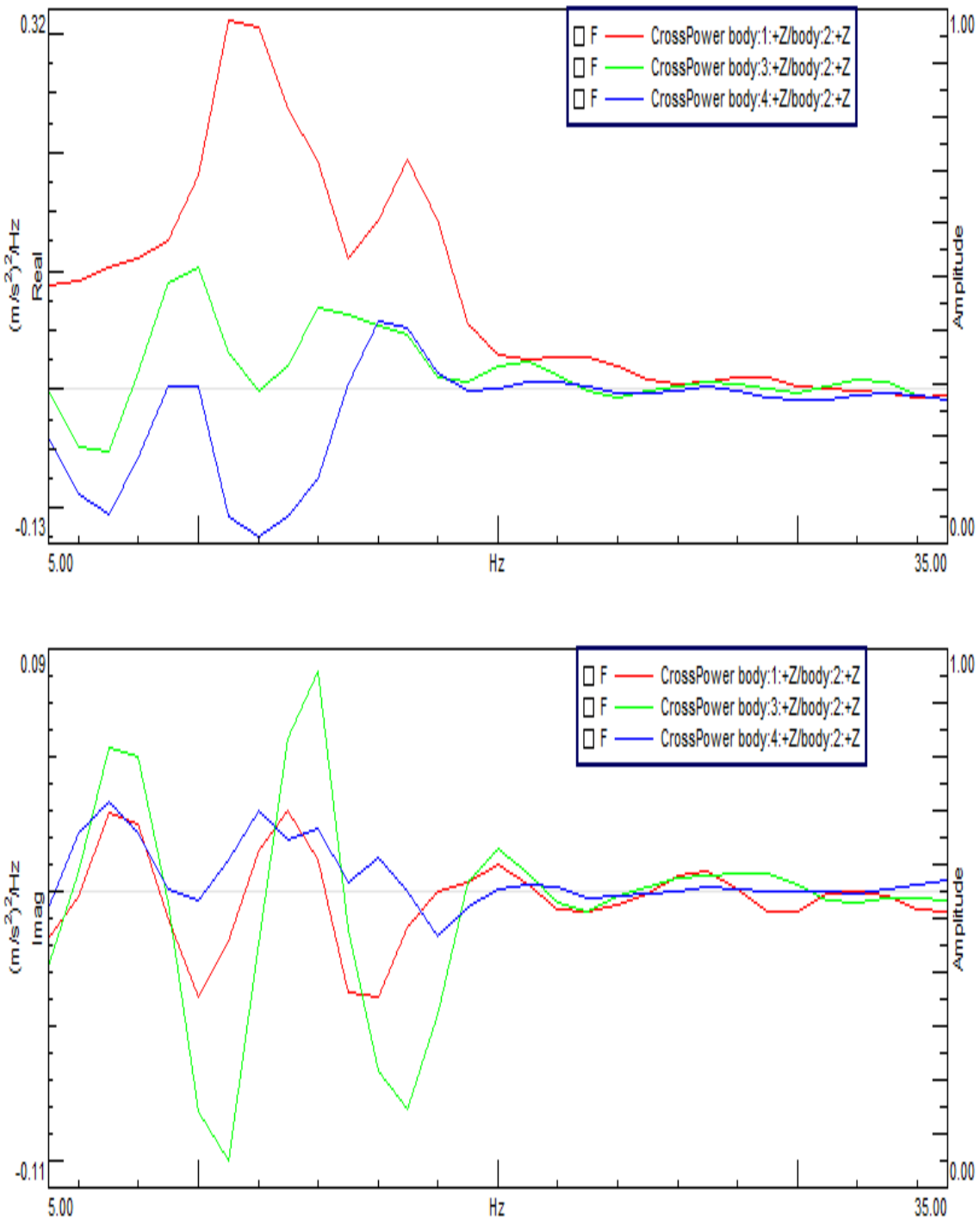

Figure 37: Cross PSD about point Two

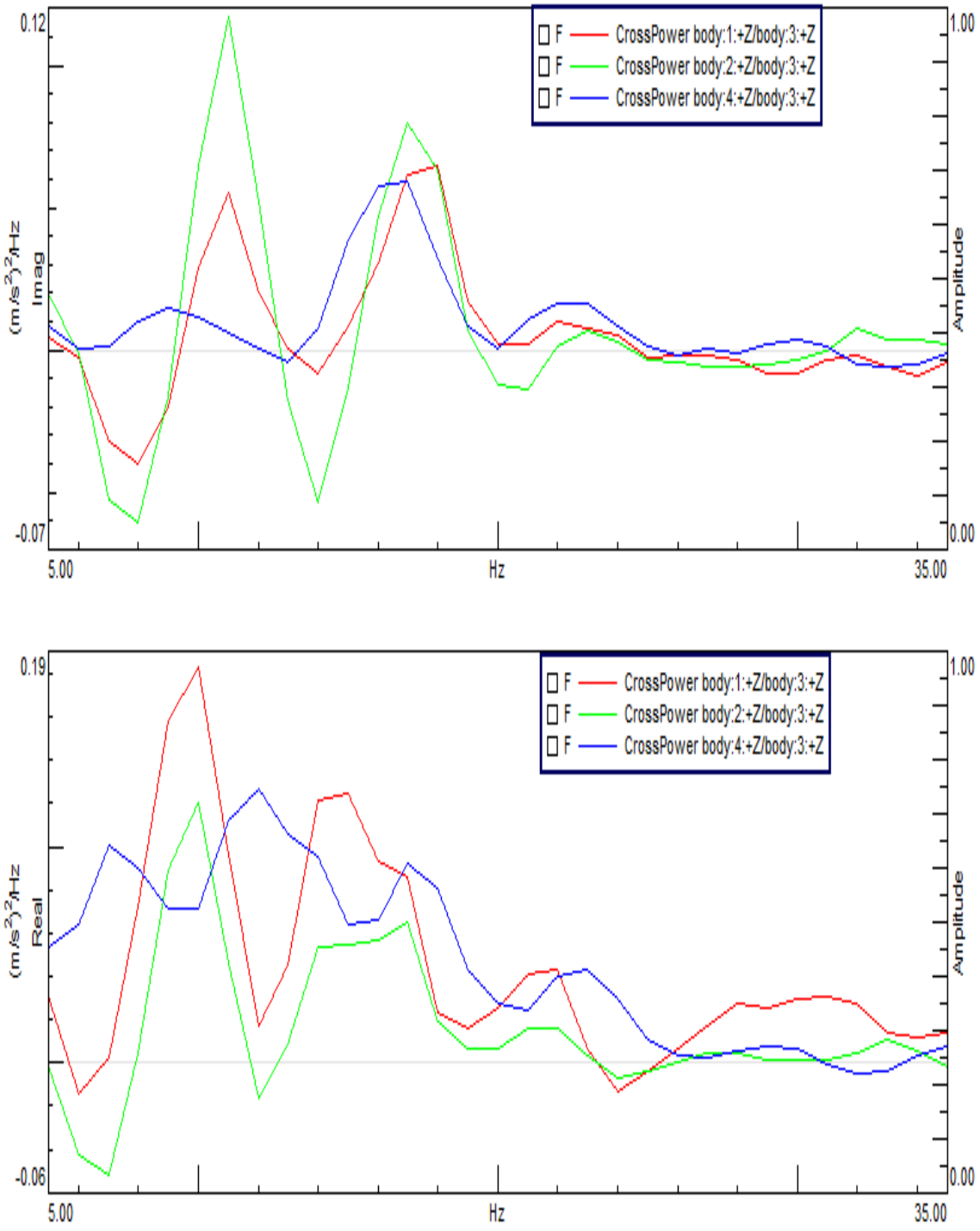

Figure 38: Cross PSD about point three

4.3 Results for response location under random road excitations

Physically this point is the middle point at top most of the engine hood panel structure. This location is important from driver's view as it shows the most obvious flutter response. Furthermore, compared with the other points at top of the panel, the highest amplitudes of vibration response under low speed road excitation occur at this point.

The second objective of this work is to find the response of the structure at the location of interest under the random road profile. The last two graphs show the trends of response in frequency domain.

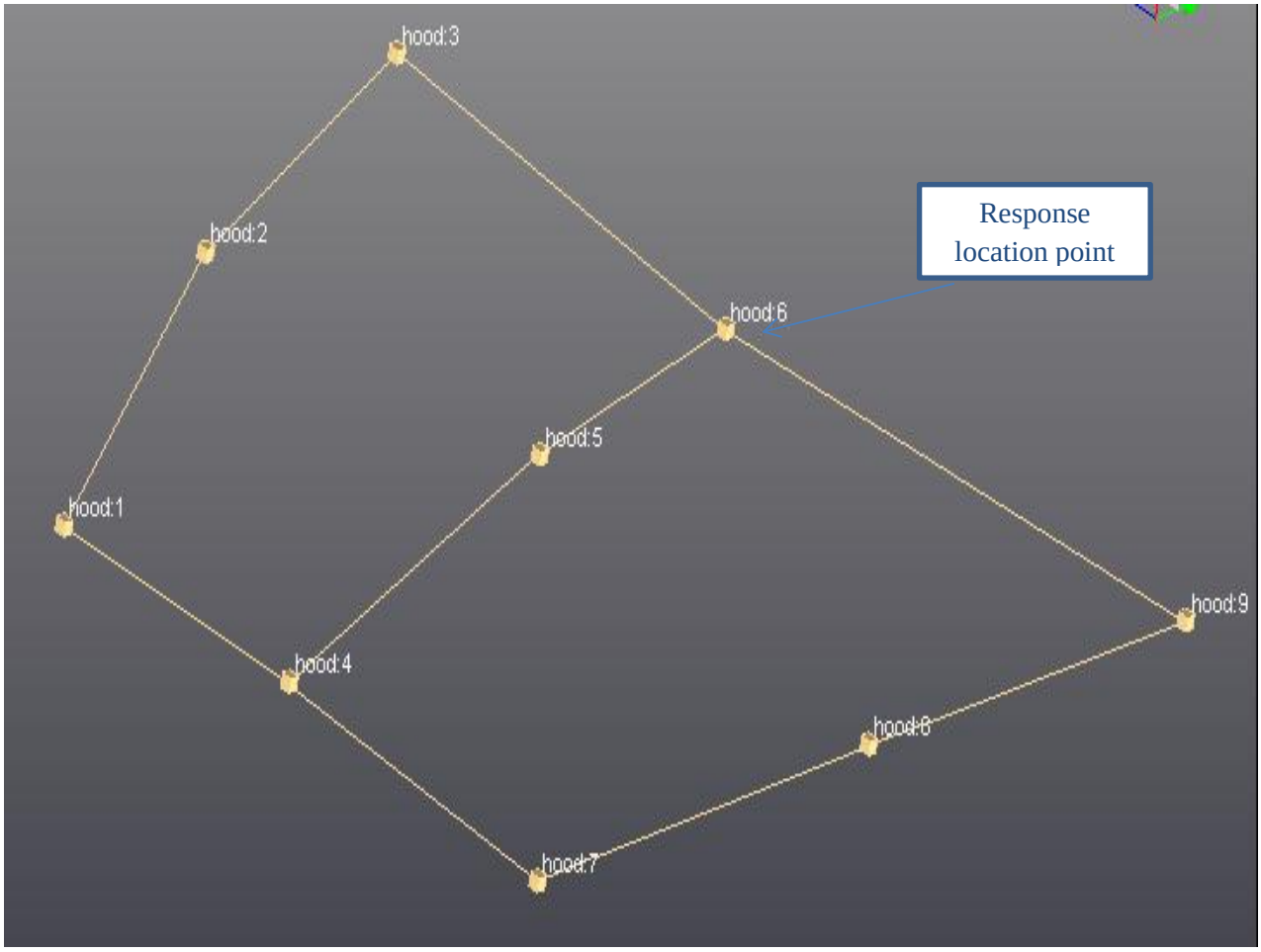

Figure 39: Response location of the structure

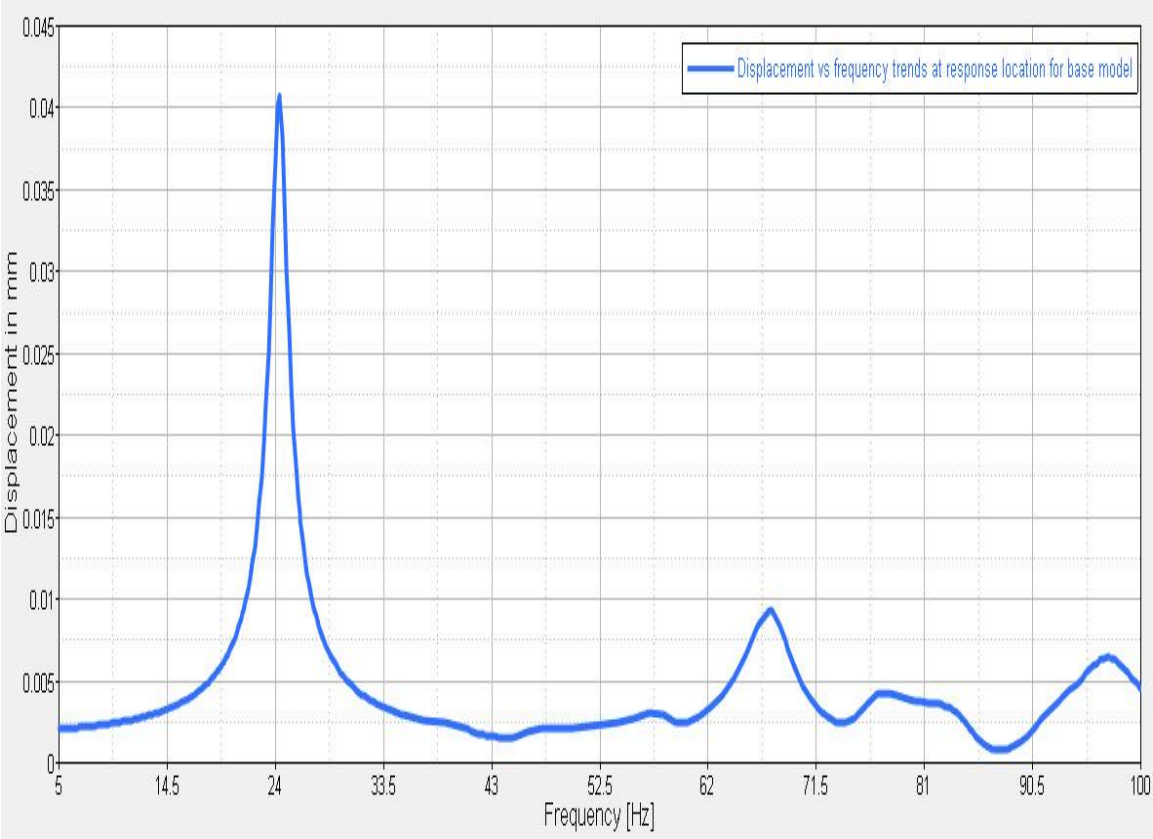

Figure 40: Response graph at the point of interest

CHAPTER 5 SUPPRESSION OF ENGINE HOOD VIBRATION RESPONSE

Finding response displacements at the point of interest in the previous chapter, this chapter is dedicated to lowering the response amplitudes at designated locations.

Based on what have been reviewed in chapter two, in order to reduce the vibration levels, different methods are used. Damping materials, introducing curvature, stiffening ribs or beads are some of these techniques which are based on increasing stiffness of the structure. The main concern is that these methods are only applicable in the earlier stage of development as modifications on sheet metal work are possible. However in the latest development process, they are not at all feasible as no changes in the geometry is allowed. One remedy is to adding stiffness to the structure through changing the stiffness of over-slam and primary bumpers. This technique is studied in this chapter. For this purpose, fifth iterations are presented. The iterations Start from increase of 50% up to 150% in increment of 25% in stiffness of bumpers.

Figure 41: Samples for over slam bumpers, Used in Hyundai and Jeep vehicles

5.1 Iterations to find the optimum values of the response

As can be seen from Figure 41, it seems that only first and third resonances are excited by the road roughness. Increasing the stiffness of bumpers rom 50% up to 150% affect the response of the structure to the road excitations. These trends are illustrated in Figure 43.

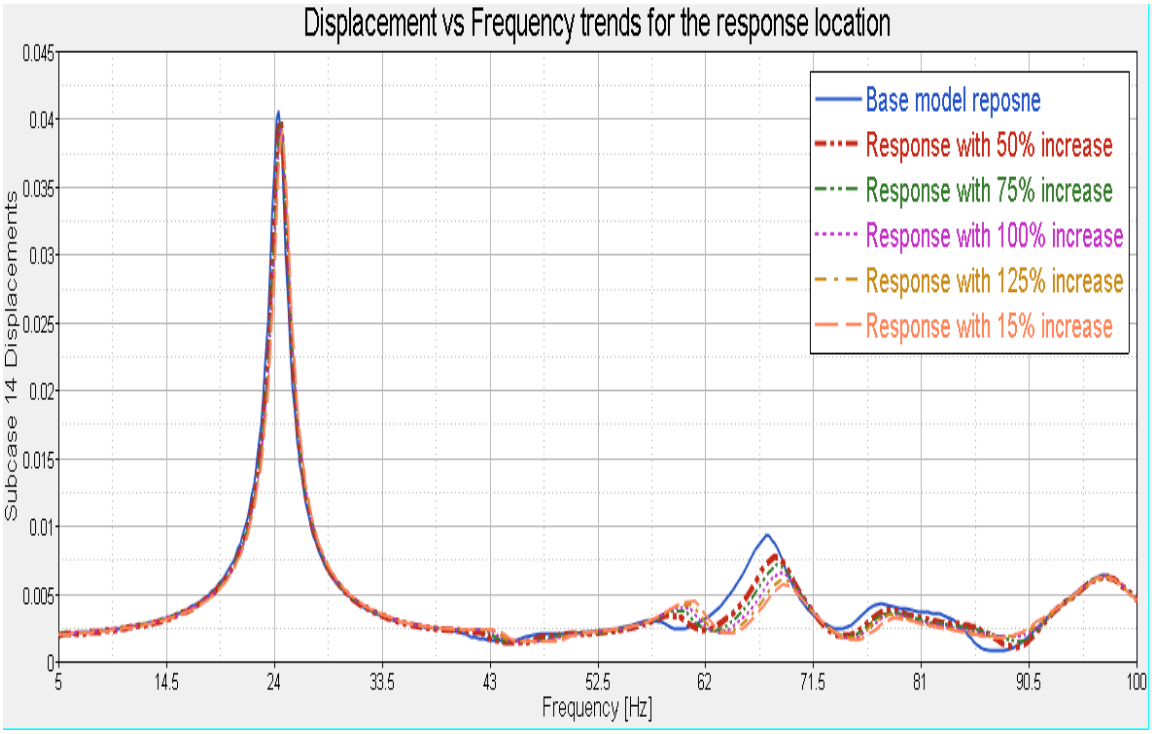

Figure 42: Response of the model with increase in stiffness of bumpers

Obviously this technique has greater impacts on the third mode at 68 Hz rather than the first. The details are shown in the Tables 5.1 and 5.2. Table 5.1 tabulates the contribution of bumpers stiffening on the response amplitudes.

Table 5. 1: Contribution of stiffening of bumpers to response amplitude

Increase in stiffness%	0	50	75	100	125	150
First Peak amplitude in mm	0.041	0.040	0.040	0.040	0.039	0.039
Difference with the base model	-	-2.5%	-2.5%	-2.5%	-5%	-5%
Second Peak amplitude in mm	0.009	0.008	0.007	0.007	0.006	0.006
Difference with the base model%	-	-11%	-22%	-22%	-33%	-33%

The influence of stiffening bumpers to peak frequencies of the structure is studied in table 5.12.

Table 5. 2: Contribution of stiffening of bumpers to response amplitude

Stiffness increase %	First peak	Difference with base model	Third peak	Difference with base model
0	24.3Hz	-	67.3 Hz	-
50	24.5 Hz	1.1%	68.1Hz	1.5%
75	24.6Hz	1.2%	68.3 Hz	1.5%
100	24.6 Hz	1.2%	68.5 Hz	1.8%
125	24.7 Hz	1.6%	68.7 Hz	2.1%
150	24.7 Hz	1.6%	68.9 Hz	2.4%

Increasing stiffness slightly reduces the amplitudes of the first mode. However, it has a significant effect on the third mode. And also according to Figure 43, by increasing the stiffness the peak at third resonance splits to two peaks and a valley.

All in all, increasing the stiffness of the elastic bumpers decreases the amplitudes of vibration responses. This change is not very significant at the first mode but very noticeable on the third mode. Interesting point is that almost no considerable frequency shift is observed while stiffening the bumpers. Convenient cost of this modification and also its accessibility throughout all the development process along with exerting not a significant shift of natural frequencies of the system are the main advantages of this method. Needless to say, using damping layers or tuned mass absorbers are not tangible in latest stage of development of engine hood structure. Introducing curvature, bead or ribs are other methods to reduce the vibrations which are only applicable in the very earliest stage of development.

CHAPTER 6 CONCLUSIONS

This work provides metrics of hood flutter under random road excitations. Validation of CAE results with those of EMA was first studied. Hinges and bumpers are constraint in all directions but latches are only constrained in the translational indirection of Y and Z axes. Another method is to remove all the constraints except for rotational Y and Z. Both methods led to similar results for mode shapes and natural frequencies. It was observed that the first resonance happens at 24 Hz and is bending (oil-canning) about the Z axis. The second mode which is torsional occurs at 45.6 Hz. In almost the same pattern but at different amplitudes, at 66.9 and 80 Hz a bending and a torsional mode occur, respectively.

After validating the CAE model, random vibration analysis was applied to find the structure response under road surface unevenness. In order to present the severity of the road profile, four accelerometers were installed at four points to get the PSD coming from the road to the structure. The input of the analysis was the PSD (frequency varying accelerations) in four points along with their cross-correlation effects on each other. The velocity of the vehicle remained constant during the experiment for being a stationary process. The system was the CAE model validated through the previous step. The output was the response amplitude of one point of the structure. This point was located at the topmost of the structure in the middle experiencing the highest fluctuations from the driver's view.

A common method to reduce the amplitude of a vibratory system is to increase the stiffness of the structure. This can be achieved by introducing curvature, stiffening bead

or ribs to the panel which are available in the early stages of design and considered as an expensive solution. Moreover, they work efficiently in damping the first mode vibration level but may have adverse effects on the radiated noise and also vibrations at other modes. The technique adopted in this work was to focus on the effect of elastic bumpers on suppressing the hood oscillations. They are reasonably inexpensive and easy-to-use at every stage of design and development. The only thing that must be checked is to ensure that the hood structure is still easy to open and close. Furthermore, even an increase of stiffness to more than twice the initial values does not shift the frequency more than 2.4%. Different iterations starting from increase of 50% in stiffness of bumpers up to 150% revealed that the amplitude of response was inversely proportional to the stiffness factors. While the first mode was dampened slightly the higher modes reacted more significantly. It is interesting to note that no increase in vibration levels was observed in the modes below 80 Hz unlike the utilization of beads or ribs.

6.1 Future works

The current research suggests developing an analytical model to represent the hood geometry based on an integrated aluminum panel and also considering the inner and outer panels as composite structures. Due to its curvature, a shell model is likely to match well with the actual physique. The results of CAE, mathematical and Experimental Modal Analyses can be used to compare and evaluate the different approaches.

Furthermore, the random excitations of road can be modelled mathematically by the methods described in Chapter 1 and the obtained response can be compared with the

experimental results. The road surface roughness can also be measured directly by laser and the results can be used as input data for running random analysis in CAE.

Finally, the nonlinearities regarding latches, hinges and bumpers can be the subject of further studies. For instance, the effect of changing the stiffness of the bumpers can be studied experimentally on road and compared with the results obtained from this work.

REFERENCES

[1] Gaylard, A. P., Beckett, M., Gargoloff, J., and Duncan, B., 2010, "CFD-based modelling of flow conditions capable of inducing hood flutter," SAE Technical Papers , No: 2010-01-1011, pp. 675-680.

[2] Gupta, A., Gargoloff, J., and Duncan, B. D., 2009, "Response of a prototype truck hood to transient aerodynamic loading," SAE International Journal of Commercial Vehicles, 2(1), pp. 75-87.

[3] Duonian, Y., Luyao, Z., Li, L., and Zhengcai, H., 2012, "Optimization of hood thickness based on the multi-objective," Applied Mechanics and Materials 197, pp. 755-759.

[4] Quinman, F., and Yonghai, W., 2011, "Random Vibration Simulation of a Special Truck Frame Based on FEM," Advanced Materials Research, 282-283, pp. 629-632.

[5] Rustighi, E., Elliott, S. J., Finnveden, S., Gulyas, K., Mocsai, T., and Danti, M., "Linear stochastic evaluation of tyre vibration due to tyre/road excitation," Proc. The 6th European Conference on Noise Control: Advanced Solutions for Noise Control, p. 6.

[6] Mucka, P., 2004, "Road waviness and the dynamic tyre force," International Journal of Vehicle Design, 36(2-3), pp. 216-232.

[7] Lakusic, S., Bogut, M., and Simun, M., "Vehicle vibrations due to road surface roughness in urban areas," Proc. Institute of Noise Control Engineering of the USA - 23rd National Conference on Noise Control Engineering, pp. 421-430.

[8] Kuijpers, A., "Towards silent tracks and roads: Beating the roughness," Proc. Forum Acusticum Budapest 2005: 4th European Congress on Acustics, pp. 1159-1164.

[9] Schiehlen, W., 2006, "White noise excitation of road vehicle structures," Sadhana - Academy Proceedings in Engineering Sciences, 31(4), pp. 487-503.

[10] Kropac, O., and Mucka, P., 2009, "Classification scheme for random longitudinal road unevenness considering road waviness and vehicle response," Shock and Vibration 16(3), pp. 273-289.

[11] Ramji, K., Gupta, A., Saran, V. H., Goel, V. K., and Kumar, V., 2004, "Road roughness measurements using PSD approach," Journal of the Institution of Engineers (India): Civil Engineering Division, 85(2), pp. 193-201.

[12] Ahlin, K., Granlund, J., and Lindstrom, F., 2004, "Comparing road profiles with vehicle perceived roughness," International Journal of Vehicle Design, 35(2-3), pp. 270-286.

[13] Razvan, C., and Iulian, L., 2013, "Random excitation of a car component from the road," Applied Mechanics and Materials, 430, pp. 184-190.

[14] Kropac, O., and Mucka, P., 2008, "Effect of obstacles in the road profile on the dynamic response of a vehicle," Proceedings of the Institution of Mechanical Engineers, Part D: Journal of Automobile Engineering 222(3), pp. 353-370.

[15] Safaei, M., Azadi, S., Keshavarz, A., and Zahedi, M., 2014, "The refinement of a vehicle NVH performance by optimizing sub-frame mounts," SAE Technical Papers , No: 2014-01-1692.

[16] Garcia, R., Manuel, A., and Rouillard, V., 2001, "On the statistical distribution of road vehicle vibrations," Packaging Technology and Science 24(8), pp. 451-467.

[17] Rouillard, V., Sek, M. A., and Bruscella, B., 2001, "Simulation of road surface profiles," Journal of Transportation Engineering, 127(3), pp. 247-253.

[18] Qin, Y., Guan, J., and Gu, L., 2012, "The research of road profile estimation based on acceleration measurement," Vibration, Structural Engineering and Measurement II 226-228, pp. 1614-1617.

[19] Lu, F., Kennedy, D., Williams, F. W., and Lin, J. H., 2008, "Symplectic analysis of vertical random vibration for coupled vehicle-track systems," Journal of Sound and Vibration 317(1-2), pp. 236-249.

[20] Xu, W. T., Lin, J. H., Zhang, Y. H., Kennedy, D., and Williams, F. W., 2009, "Pseudo-excitation-method-based sensitivity analysis and optimization for vehicle ride comfort," Engineering Optimization 41, pp. 699-711.

[21] Xu, W., Miao, T., and Liu, Z., 2011, "An Efficient Multi-objective Optimization Method for Complicated Vehicle Random Vibration," Applied Mechanics and Materials 94-96, pp. 1694-1700.

[22] Zhang, Y., and Jiang, M., "Random vibration analysis and parameter optimization," Proc. Proceedings of the Annual Reliability and Maintainability Symposium, pp. 217-221.

[23] Dahlberg, T., 1977, "Parametric optimization of a 1-DOF vehicle travelling on a randomly profiled road," Journal of Sound and Vibration 55(2), pp. 245-253.

[24] Tang, X., and Zuo, L., 2012, "Vibration energy harvesting from random force and motion excitations," Smart Materials and Structures 21(7), pp. 1-9.

[25] Xu, Y. L., Zhang, W. S., Ko, J. M., and Lin, H. J., 1999, "Pseudo-excitation method for vibration analysis of wind-excited structures," Journal of Wind Engineering and Industrial Aerodynamics, 83, pp. 443-454.

[26] Qin, Y., Wang, J., and Tian, G., 2011, "Random Vibration Analysis of Heavy-duty Truck Based on Pseudo Excitation," Advanced Materials Research, 299-300, pp. 1244-1247.

[27] Lu, M. H., and Jen, M. U., 2012, "Investigation and reduction of motor noise for battery electric van," 41st International Congress and Exposition on Noise Control Engineering, 3, pp. 2475-2483.

[28] Jha, A., Nikolaidis, E., and Gangadharan, S., 2000, "Vibration of dynamic systems under cyclostationary excitations," AIAA journal 38(12), pp. 2284-2291.

[29] Cryer, B. W., Nawrocki, P. E., and Lund, R. A., 1976, "A road simulation system for heavy duty vehicles," SAE Technical Papers , No: 760361, pp. 1-5.

[30] Hassan, R., and McManus, K., 2003, "Assessment of Interaction between Road Roughness and Heavy Vehicles," Transportation Research Record II 18-19, pp. 236-243.

[31] Hesami, R., and Manus, K. J. M., "Signal processing approach to road roughness analysis and measurement," Proc. IEEE Region 10 Annual International Conference Proceedings/TENCON, pp. 1-6.

[32] Delanne, Y., and Pereira, P. A. A., 2001, "Advantages and limits of different road roughness profile signal-processing procedures applied in Europe," Transportation Research Record, 1764, pp. 254-259.

[33] Agostinacchio, M., Ciampa, D., and Olita, S., 2013, "The vibrations induced by surface irregularities in road pavements - a Matlab® approach," European Transport Research Review, pp. 1-9.

[34] Gillespie, T. D., and Karamihas, S. M., 2000, "Simplified models for truck dynamic response to road inputs," Heavy Vehicle Systems 7(2-3), pp. 231-247.

[35] Sujitamo, B., 1991, "Human perception response of vehicle excited by random road roughness," Proceedings of the 6th International Pacific Conference on Automotive Engineering pp. 1165-1172.

[36] Barbosa, R., 2011, "Vehicle dynamic response due to pavement roughness," Journal of the Brazilian Society of Mechanical Sciences and Engineering 33(3), pp. 302-307.

[37] Otat, V., 2005, "Mathematical algorithms used to study the vibrations of car bodywork elements," European Automobile Engineers Cooperation - 10th EAEC European Automotive Congress, 1, pp. 463-467.

[38] Wu, Y., and Fan, Q., 2011, "Modeling and simulation of truck with random vibration response," 6th International Conference on Computer Science & Education (ICCSE 2011), pp. 452-455.

[39] Kido, I., Ueyama, S., Hashioka, M., Yamamoto, S., Tsuchiyama, M., and Yamaoka, H., 2011, "Tire and Road Input Modeling for Low-Frequency Road Noise Prediction," SAE International Journal of Passenger Cars - Mechanical Systems 4(2), pp. 1277-1282.

[40] Mucka, P., and Kropac, O., 2009, "Sensitivity of road unevenness indicators to road waviness," Journal of Testing and Evaluation 37(2), pp. 139-149.

[41] Munari, L. A., Fontanella, L., Hoss, L., and Marczak, R. J., 2012, "Retrieving road surface profiles from PSDs for ride simulation of vehicles," SAE Technical Papers , No: 2012-36-0003.

[42] Xu, D. M., Mohamed, A. M. O., Yong, R. N., and Caporuscio, F., 1992, "Development of a criterion for road surface roughness based on power spectral density function," Journal of Terramechanics 29(4-5), pp. 477-486.

[43] Mann, A. V., Mcmanus, K. J., and Holden, J. C., 1997, "Power spectral density analysis of road profiles for road defect assessment," Road and Transport Research 6(3), pp. 36-46.

[44] Borowiec, M., Sen, A. K., Litak, G., Hunicz, J., Koszaka, G., and Niewczas, A., 2010, "Vibrations of a vehicle excited by real road profiles," Forschung Ingenieurwesen/ Engineering Research, 74(2), pp. 99-109.

[45] Hanouf, Z., Faris, W. F., and Nor, M. J. M., 2014, "Dynamic characterization of car door and hood panels using FEA and EMA," Applied Mechanics and Materials, 471, pp. 89-96.

[46] Lampas, G., Pasialis, V., Siebert, T., Feligiotti, M., and Pipino, A., 2011, "Validation of impact simulations of a car bonnet by full-field optical measurements," Applied Mechanics and Materials, 70, pp. 57-62.

[47] Siebert, T., Wang, W., Mottershead, J. E., and Pipin, A., 2011, "Application of high speed image correlation for measurement of mode shapes of a car bonnet," Applied Mechanics and Materials, 70, pp. 45-50.

[48] Saravanan, K., and Injeti, S. K., 2013, "Fuel tank finite element modeling method for accurate vibration characteristics prediction," SAE Technical Papers , No: 2013-26-0036, pp. 1-5.

[49] Hodges, D. H., and Pierce, G. A., 2011, Introduction to structural dynamics and aeroelasticity, Cambridge University Press, New York, NY.

[50] Hartley, C., 2011, "Simulating the static and dynamic response of an automotive weatherstrip component," SAE Technical Papers , No: 2011-01-1602, 4(2), pp. 1111-1125.

[51] Deng, X. L., Zhao, X. Z., and Li, l., 2005, "Vibroacoustic optimization of two cross stamped ribs in a plate," SAE Technical Papers , No: 2005-01-1067.

[52] Qian, Y., Aggrawal, A., and Khan, H., 1997, "Damping efficiency of ribbed panels with different damping materials," SAE Technical Papers , No: 971930.

[53] Tarnoczy, T., 1970, "Vibration of metal plates covered with vibration damping layers," Journal of Sound and Vibration 11(3), pp. 299-307.

[54] Onsay, T., Akanda, A., and Goetchius, G., 1999, "Vibro-acoustic behavior of bead-stiffened flat panels: FEA, SEA, and experimental analysis," SAE Technical Papers , No: 1999-01-1698.

[55] Blanchet, D., Hal, W. V., and Caillet, A., 2010, "Effect of beading on radiated noise," SAE Technical Papers , No: 2010-01-1407, 3(1), pp. 868-874.

[56] Pagnotta, L., 2003, "Structural optimization of an automotive dashboard support by genetic algorithms," WIT Transactions on the Built Environment, 67, pp. 67-74.

[57] Carfagni, M., Citti, P., Governi, L., and Pierini, M., 2004, "Vibro-acoustic optimization of stiffening ribs and damping material distribution on sheet metal parts," Shock and Vibration, 11(3-4), pp. 271-280.

[58] Maladahiyar, K., Girish, M. G., Vijay, R. C., and Mangalaramanan, S. P., 2008, "Design of wind deflector ribs using topology optimization and validation through FE analysis and testing," SAE Technical Papers , No: 2008-01-2665.

[59] Aydemir, B., and Ebrinc, A., 2009, "Effect of material properties and wall thickness of polymer based intake manifold on the engine radiated noise levels," SAE Technical Papers , No: 2009-01-0345.

[60] 2014, "(http://www.sensorprod.com/news/white-papers/2008-08_qac/index.php)."

[61] 2013, "MSC Nastran dynamic analysis user's guide," MSC Software Corporation, USA.

[62] INTERNATIONAL, L., 2011, "MODAL ANALYSIS."

[63] 2014, "www.PCB.com."

ABSTRACT

ANALYSIS AND SUPPRESSION OF ENGINE HOOD VIBRATIONS UNDER RANDOM ROAD EXCITATIONS

by

HOOMAN FARROKHZADEH

May 2015

Advisor: Dr. Chin An Tan

Major: Mechanical Engineering

Degree: Master of Science

Vehicle designs and developments must meet safety legislations along with market demands. Safety regulations are mainly concerned with how a vehicle body performs in crashes, during which pedestrian collision is the one of the most important issues. When a vehicle strikes a pedestrian, its engine hood will most likely hit the head of the pedestrian, causing serious injuries. To reduce the severity of the injuries, along with market demands to improve vehicle fuel economy and performance, engineers have considered the design solution of reduction of the vehicle hood thickness (and hence its weight) and the use of advanced light materials. As a result, the engine hood panel becomes much more susceptible to excessive vibrations. The sources of these vibrations are road irregularities which provide base excitations and aerodynamic fluid-structure interactions.

Engine hood vibrations due to aeroelasticity, called flutter, have been investigated extensively in the past using CAE, wind tunnel experiments, and modeling and simulations by computational fluids dynamics (CFD) techniques. This work studies engine hood vibrations due to excitations from road surface irregularities and explores a passive technique to suppress the levels of vibrations. Due to the unpredictable nature of surface irregularities, this problem is approached by random vibrations analysis. Validated CAE model, with experimental modal analysis, and random vibration analysis are employed to determine the system response under road excitations. The power spectral densities (PSD) of road irregularities are obtained by experiments and used as inputs to the vibratory system. Finally the effects of stiffening elastic bumpers on the engine hood are examined a possible passive technique to suppress vibrations. It is shown that stiffening of the elastic bumpers decreases the vibration levels for the first mode slightly but drastically in other modes. It is also observed that there is less than 2.5% shift in the frequency while increasing the stiffness of the elastic bumpers. Finally, although a suppression of less than 5% in the response amplitude of the first mode of the engine hood system might not seem significant, the proposed approach represents a plausible design solution as it is relatively simple cost-effective, and without much changes to the resonant frequencies.

AUTOBIOGRAPHICAL STATEMENT

My name is Hooman Farrokhzadeh pursuing my master's degree in Mechanical Engineering. As I started my program at Wayne State University I thought that Noise, Vibrations and Acoustics field is the toughest topic in Mechanical engineering field. The first course I took with Professor Wu on industrial noise control really motivated me to go further in this field. He taught me the concept and physics of acoustics in a very systematic approach and it has become one of my fields of interest so far. I went for a course on Vibrations with Professor Tan the next semester which really built the required fundamentals I need in Vibrations. Meanwhile having a chance to be professor Ibrahim's assistant in undergraduate vibration course, I found the marvelous opportunity of learning the basics of research. Meanwhile, courses pertaining to FEM at WSU helped me with building up proficiency FEM theory and software codes applications. Then I applied for positions in NVH field and found my chance in working with a world class car company in the USA. This work is all based on what I learnt in the period of studying at WSU and my internship program.

Once again, I would like to express my sincere appreciation to Dr. Tan, Dr. Ibrahim, Dr. Wu and Dr Singh and all my mentors and friends at WSU who helped me complete my master's program in the best possible way.